QSHS Lecture 1
Introduction to Axion Haloscopes
QTFP School 2023
10/01/23

I. Bailey
(i.bailey@lancaster.ac.uk)

Quantum Sensors for the Hidden Sector

- The development of novel, sensitive quantum electronics.
- Collaborative work the ADMX collaboration.
- Theoretical work on hidden sector phenomenology and quantum systems theory underlying quantum measurement in the hidden sector.

UNIVERSITY OF CAMBRIDGE

Lancaster University

The University Of Sheffield.

NPL National Physical Laboratory

UNIVERSITY OF OXFORD

ROYAL HOLLOWAY UNIVERSITY OF LONDON

UNIVERSITY OF LIVERPOOL

UCL

https://qshs.org/

Introduction

- A major aim of the Quantum Sensors for the Hidden Sector (QSHS) collaboration is to develop quantum technologies to increase the sensitivity of axion haloscopes, but what is an axion haloscope and what are they for?
- This lecture focuses on axions and the experimental approaches to their detection in the micro-eV mass regime.
- There are two significant caveats:

  1) I will focus mostly on axions, but these are not the only hidden-sector particles which QSHS aims to search for.
  2) If axions do exist they don't have to make up a large percentage of the dark matter halo, but they could, and I assume here that they do.

- Where possible I have given credit to all of the many presentations and papers that I've used in putting together these slides. Apologies for any omissions. A major source is the 17th Patras Workshop on axions, WIMPs and WISPs, 2022, Mainz.

Structure

- A reminder of the motivation for dark matter
- Review of dark matter candidates
- WISPs / FISPs (Feebly-interacting sub-eV particles)
- QCD Axions
- Axion couplings
- The axion-photon coupling
- Axion experimental detection techniques
- Axion haloscopes

- See Ed Daw's lecture later in the week for a quantum systems view of the detectors coupled to axion haloscopes.

Dark Matter Evidence

- Galactic rotation curves

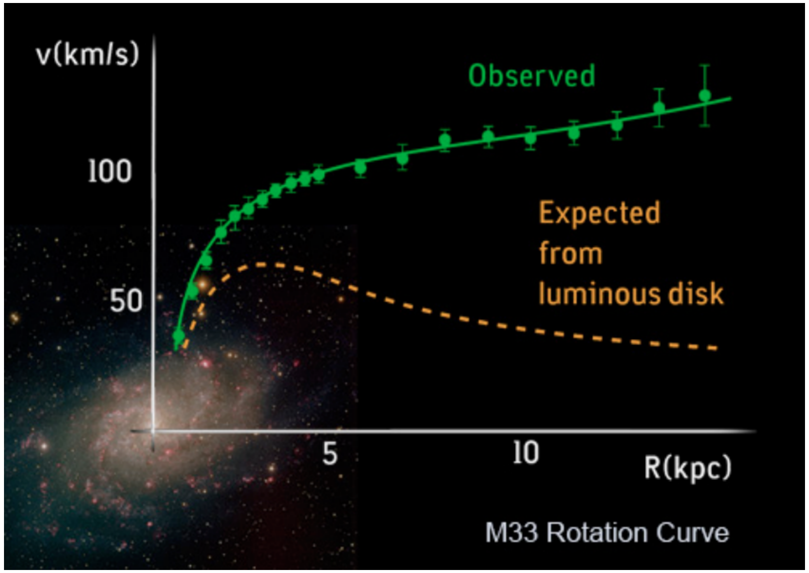

Dark Matter Evidence

- Galactic rotation curves
- Large-scale structure

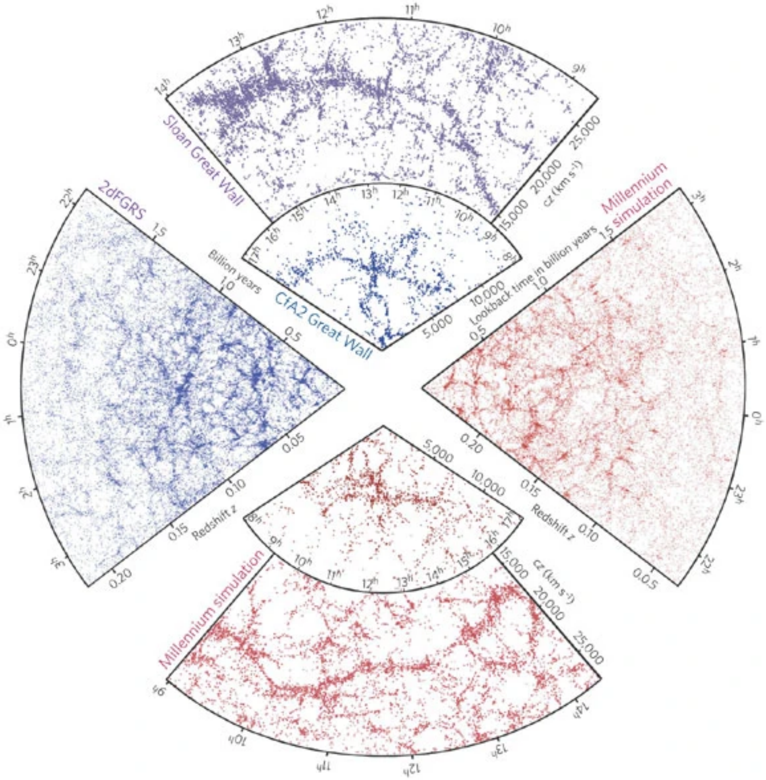

doi:10.1038/nature04805

Dark Matter Evidence

- Galactic rotation curves
- Large-scale structure
- CMB Anisotropy

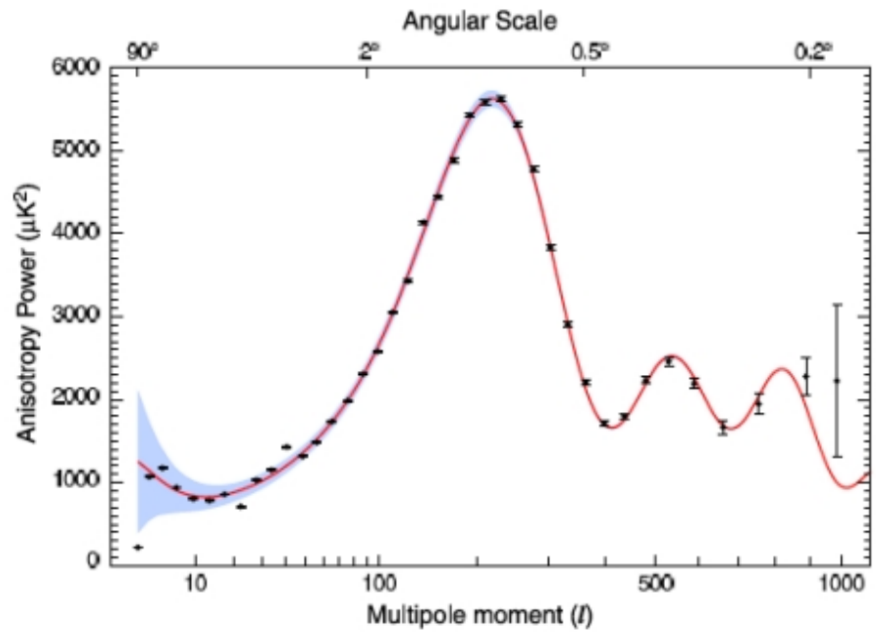

Dark Matter Evidence

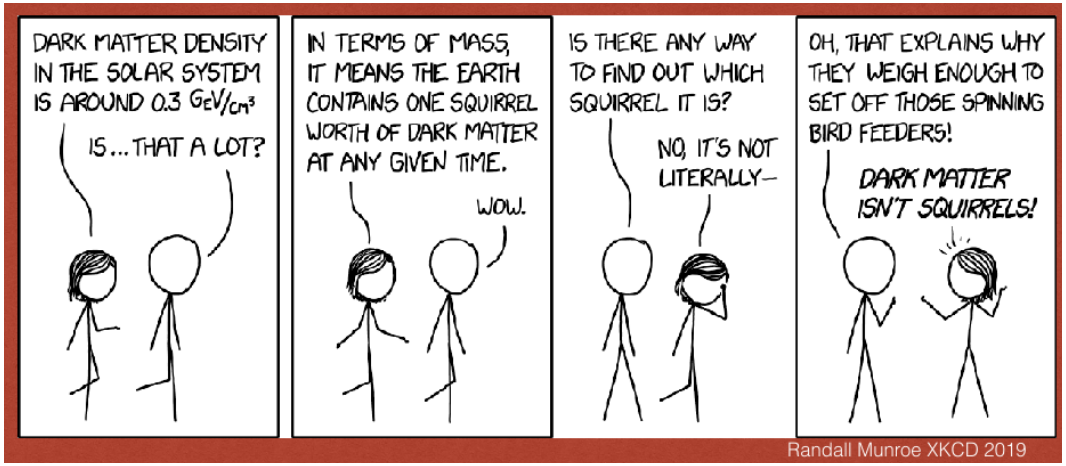

https://xkcd.com/2186

Dark Matter Evidence

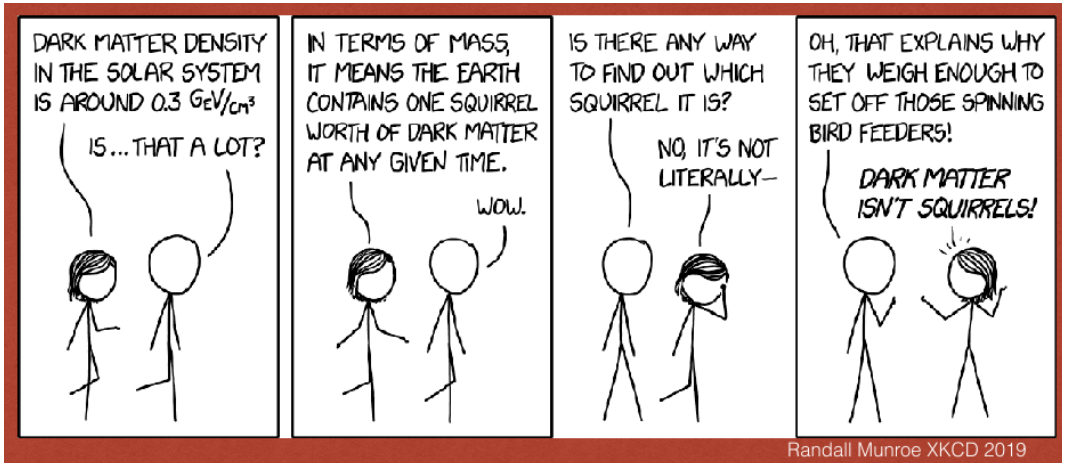

https://xkcd.com/2186

Local dark matter density is
~1 squirrel per Earth volume
~0.45 GeV cm^{-3}

Dark Matter Candidates

The dark matter candidate landscape extends from the ultralight to the very massive.

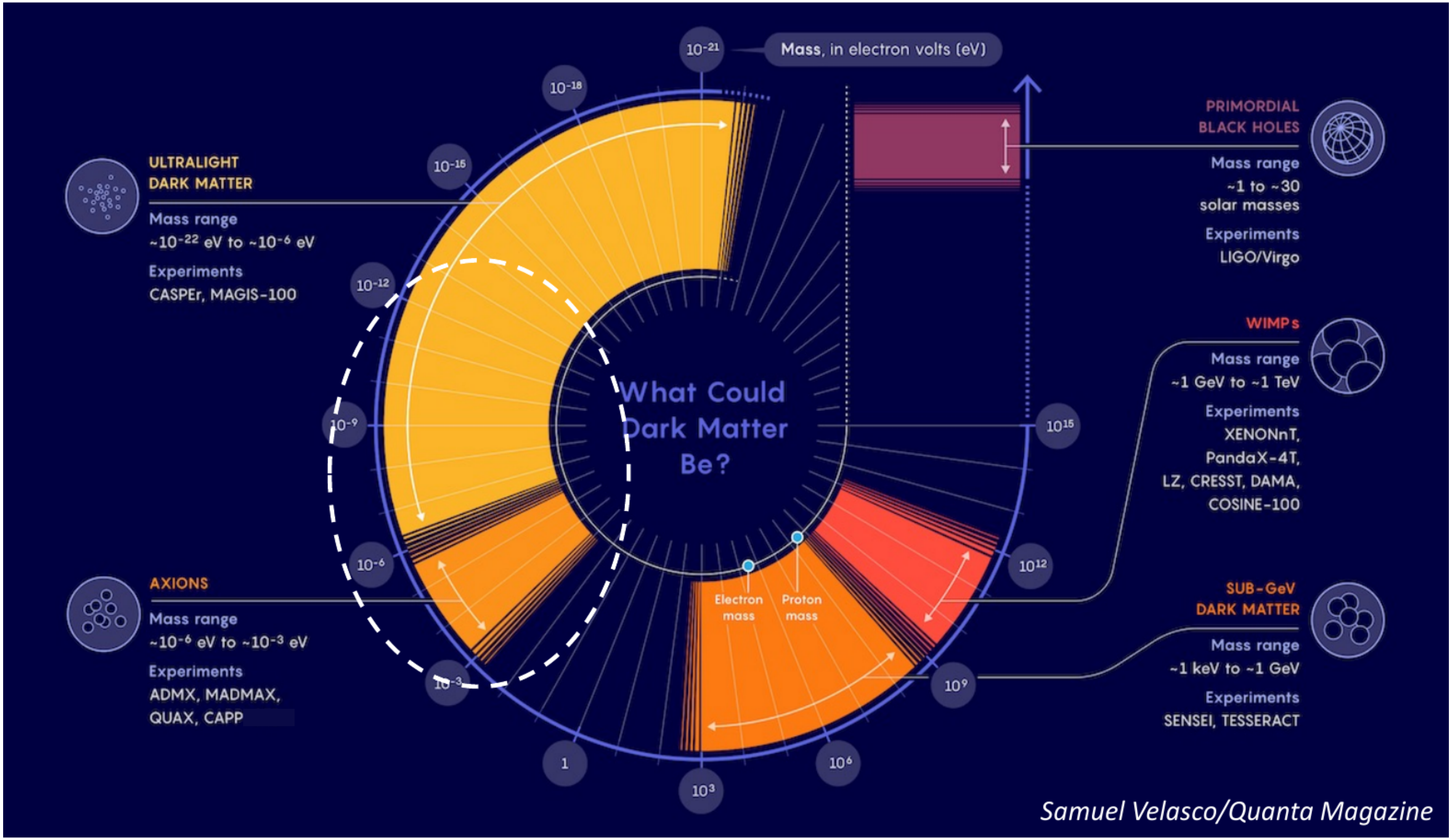

Heavy Dark Matter

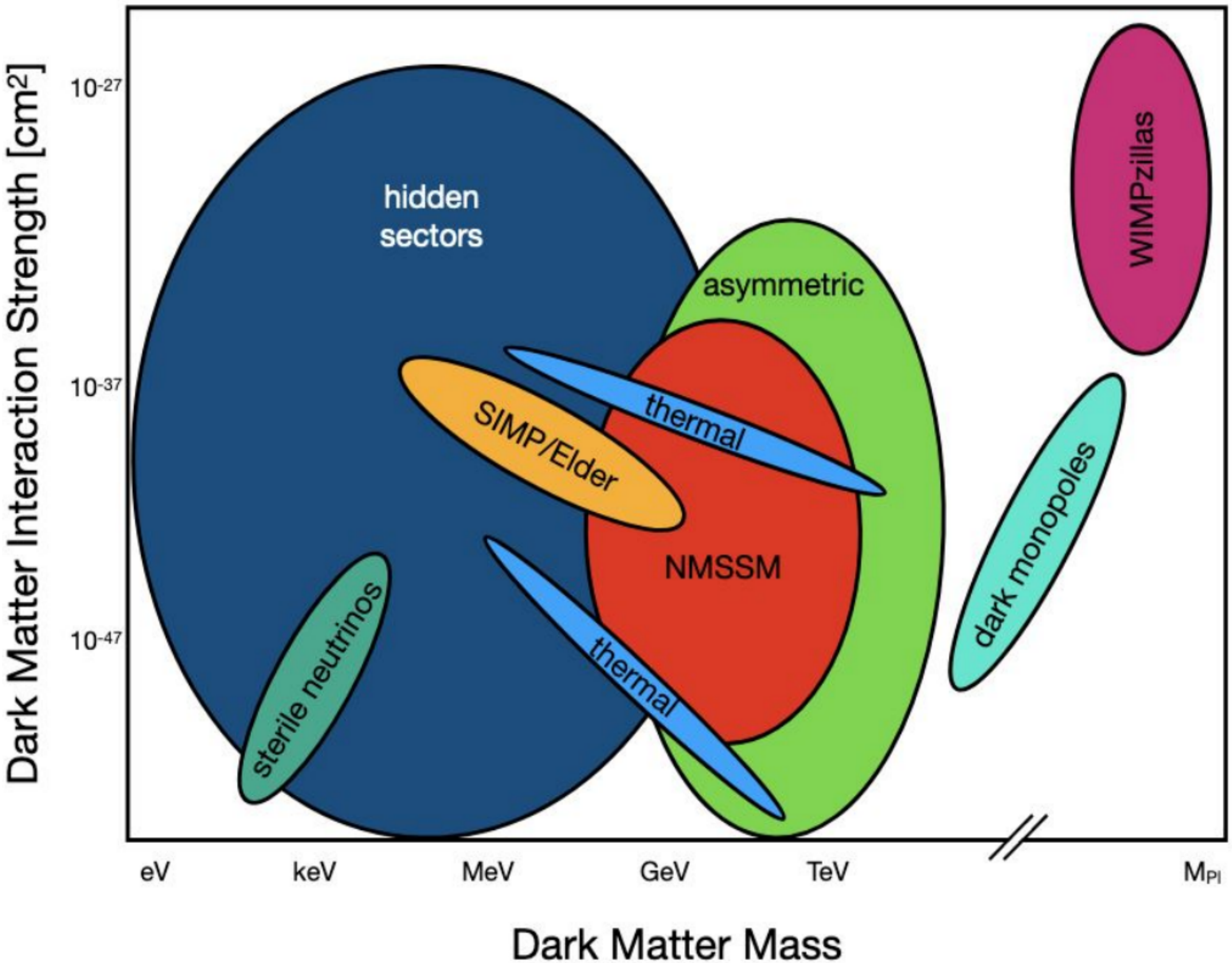

CF1 Particle Dark Matter, Convener's Report, Snowmass, 2022

Dark matter candidates are broadly described by their masses and their characteristic interaction strengths with Standard Model particles.

WISP/FISP Dark Matter

- We can also consider the spin and parity properties of potential dark matter candiates.
- Let's look specifically at Weakly (Feebly) – Interacting Sub-eV Particles

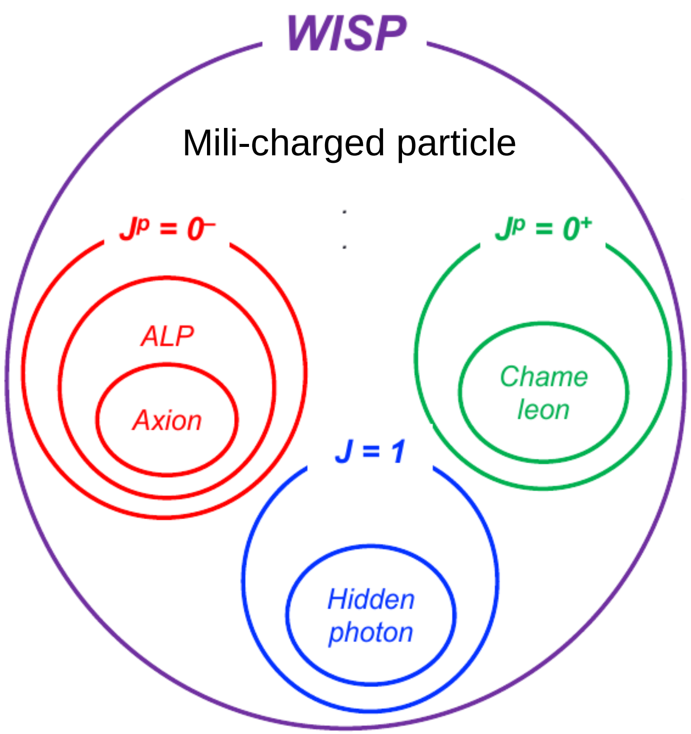

- Here we see three popular examples of WISPS classified by their spin and parity
  - Axion-like particles (ALPs)
  - Hidden-sector photons
  - Chameleons
- These are all bosons. Non-bosonic solutions are also possible, e.g. mili-charged fermions.

Bosonic Light Dark Matter Possibilities

- Below ~eV masses, dark matter behaves as an oscillating classical field.
- As before here we classify by spin and parity.

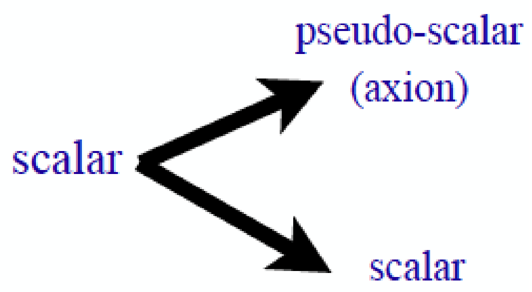

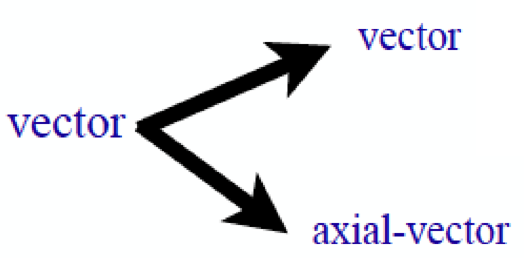

PHYSICAL REVIEW D 93, 075029 (2016)

Bosonic Light Dark Matter Possibilities

- Below ~eV masses, dark matter behaves as an oscillating classical field.
- As before here we classify by spin and parity.

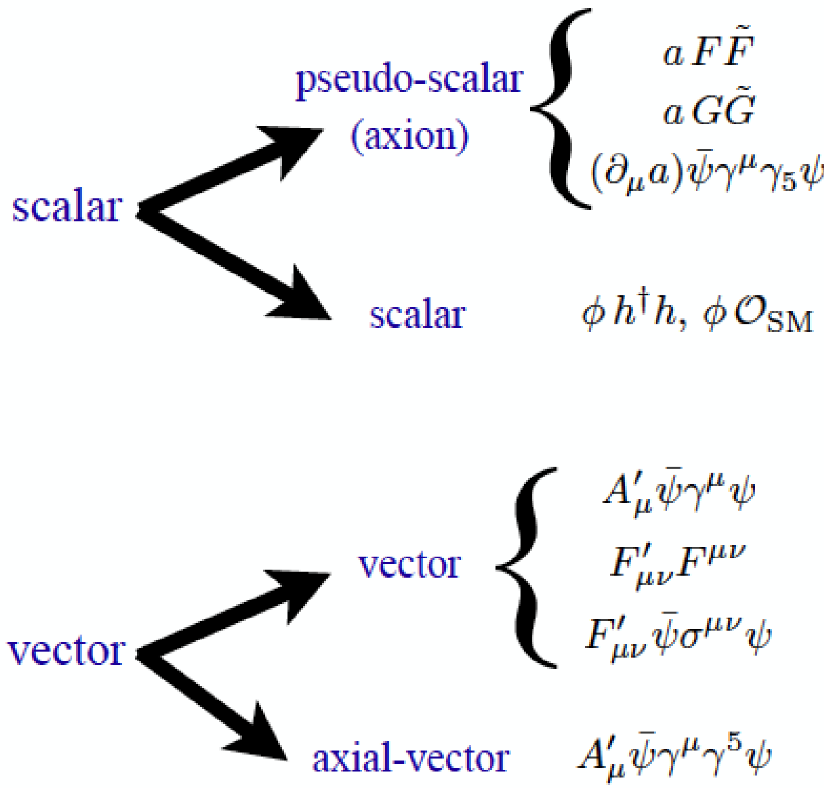

Leading order interactions, i.e. lowest dimensional operators in an effective field theory.

PHYSICAL REVIEW D 93, 075029 (2016)

Bosonic Light Dark Matter Possibilities

- Below ~eV masses, dark matter behaves as an oscillating classical field.
- As before here we classify by spin and parity.

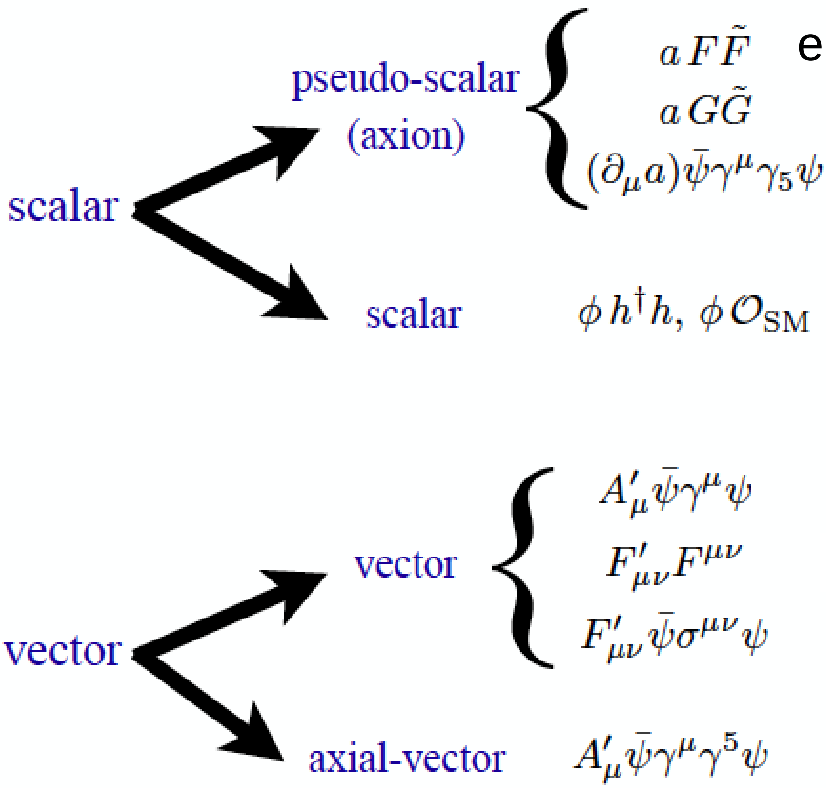

electric/magnetic fields

nuclear EDM

spin torque

e.g. electron mass

acceleration

EMF in vacuum

spin torque

spin torque

As we shall see later, the existence of these oscillating classical DM fields cause oscillations in SM observables.

PHYSICAL REVIEW D 93, 075029 (2016)

Non-pseudoscalar DM Candidates

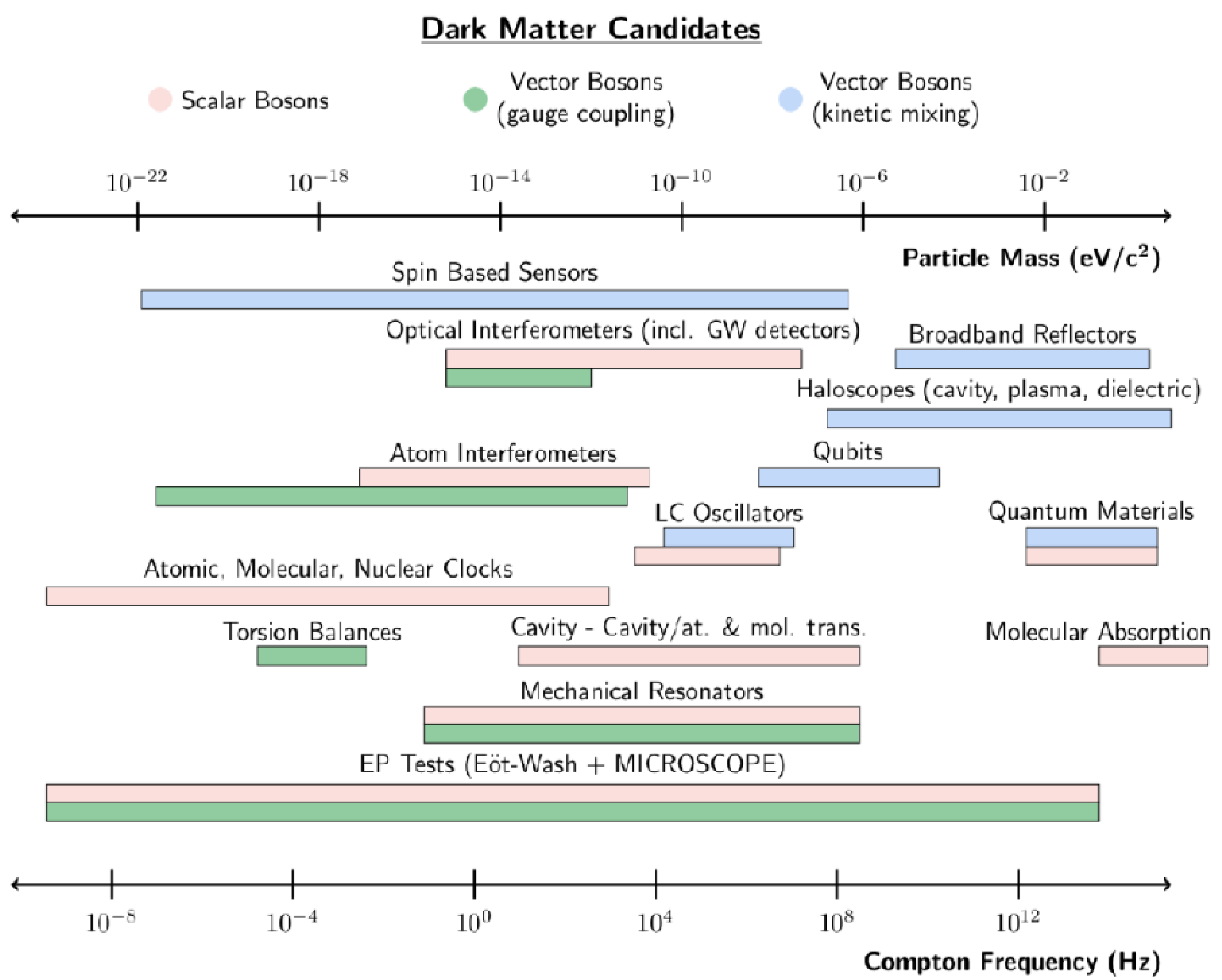

From here we will focus on pseudoscalar DM, but for completeness this figure illustrates the broad range of experimental approaches to search for scalar and vector DM candidates.

arXiv:2203.14915

The Strong CP Problem

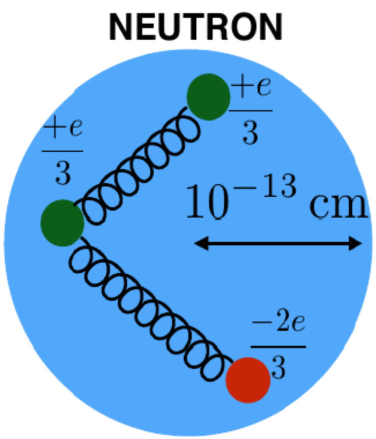

Classically, if we consider the charge distribution inside a neutron we would probably draw something similar to the diagram on the left.

The electric dipole moment is defined as

$$\vec{d} = \sum q_i \vec{r}_i$$

So we would conclude that a neutron EDM of approximately 10^{-13} e cm is natural.

However, the neutron EDM is measured experimentally (e.g. through Larmor precession measurements) to be less than 3×10^{-26} e cm.

i.e. for some reason it's as if the quarks are in a straight line…

Solutions to Strong CP Problem

- Classically there are three solutions to explain why the neutron EDM is so small.
  - Parity is a good symmetry
  - CP is a good symmetry
  - The angle between the quarks is dynamical and relaxes to zero
- A proper quantum field theory approach is beyond the scope of this lecture, but the axion solution to the strong CP problem corresponds to the third classical solution above.
- See PoS (TASI2018)004 for a full treatment.

QCD Axions

- Arise from the Peccei-Quinn solution to the strong CP problem.
- One of the terms needed in the QCD Lagrangian is

$$\theta \frac{g^2}{32\pi^2} G^{\mu\nu} \tilde{G}_{\mu\nu}$$

- This term is CP-violating, but the effect can be removed if there is also a compensating CP-violation in the quark mass matrix...
- ...but why should these two effects exactly cancel?
- Introduce a dynamical parity-violating term with a potential such that the CP-violating term is driven to zero in the ground state.

QCD Axions

- *Axion coupling to SM*

	Photons	Fermions	nEDMs
Lagrangian	$g_{a\gamma\gamma} a \boldsymbol{E} \cdot \boldsymbol{B}$	$g_{aff} \boldsymbol{\nabla} a \cdot \widehat{\boldsymbol{S}}$	$g_{EDM} a \widehat{\boldsymbol{S}} \cdot \boldsymbol{E}$
Observable (measurable)	Photon	Spin precession	Oscillating EDM
Detection	Power spectrum, photon counter, …	Magnetometer, NMR, …	NMR, polarimeter, …

In this lecture we are primarily interested In the axion-photon coupling.

Electromagnetic Field

Axion-photon coupling

$$\mathcal{L} = \boxed{J^e_\mu A^\mu - \frac{1}{4} F^{\mu\nu} F_{\mu\nu}} \boxed{+ \frac{1}{2} \partial^\mu a \partial_\mu a} - \boxed{\frac{1}{4} g_{a\gamma\gamma} a F^{\mu\nu} \tilde{F}^{\mu\nu}}$$

Axion Field

$$F^{\mu\nu} = \partial^\mu A^\nu - \partial^\nu A^\mu$$

S. Yun, 17th Patras Workshop on axions, WIMPs and WISPs, 2022, Mainz.

Primakoff Effect

Consider coupling of axion to electromagnetic fields

$$\mathscr{L}_{a\gamma\gamma} = g_{a\gamma\gamma} a \mathbf{E} \cdot \mathbf{B}$$

The effective coupling depends on the particles to which the axion can couple directly

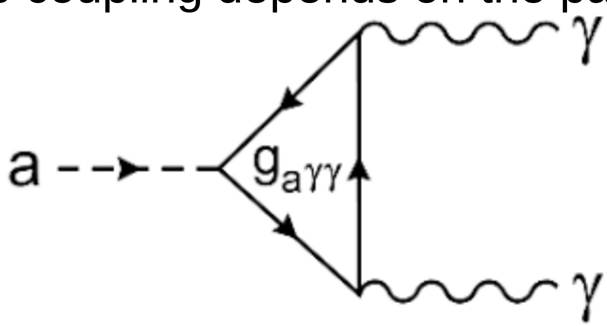

The other well-known pseudoscalar in the Standard Model is the neutral pion

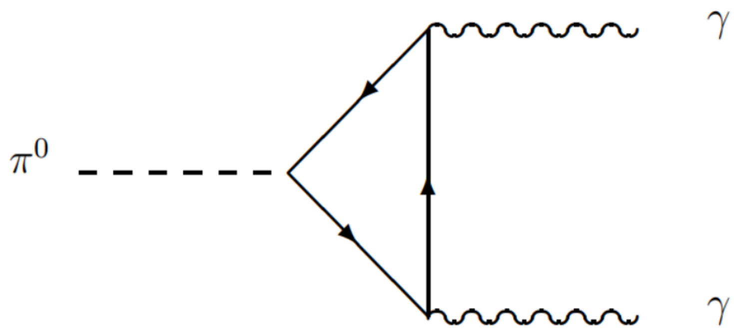

Axionic Maxwell Equations

$$\nabla \cdot \mathbf{E} = \rho - g_{a\gamma\gamma} \mathbf{B} \cdot \nabla a,$$

$$\nabla \cdot \mathbf{B} = 0,$$

$$\nabla \times \mathbf{E} = -\frac{\partial \mathbf{B}}{\partial t},$$

$$\nabla \times \mathbf{B} = \frac{\partial \mathbf{E}}{\partial t} + \mathbf{J} - g_{a\gamma\gamma}\left(\mathbf{E} \times \nabla a - \frac{\partial a}{\partial t} \mathbf{B} \right).$$

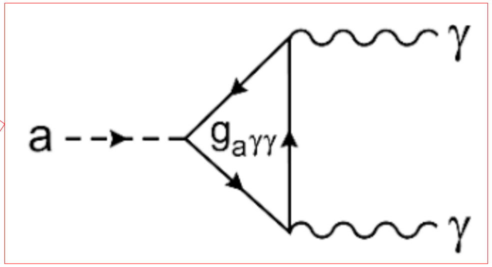

PRD99 055010 (2019)

Axionic Maxwell Equations

$$\nabla \cdot \mathbf{E} = \rho - g_{a\gamma\gamma} \mathbf{B} \cdot \nabla a,$$

$$\nabla \cdot \mathbf{B} = 0,$$

$$\nabla \times \mathbf{E} = -\frac{\partial \mathbf{B}}{\partial t},$$

$$\nabla \times \mathbf{B} = \frac{\partial \mathbf{E}}{\partial t} + \mathbf{J} - g_{a\gamma\gamma}\left(\mathbf{E} \times \nabla a - \frac{\partial a}{\partial t}\mathbf{B}\right).$$

PRD99 055010 (2019)

The axion field time-dependence $a(t, \vec{r}) = a_0 \cos(\vec{k}_a \cdot \vec{r} - \omega_a t)$

gives an effective current proportional to an applied magnetic field.

Axionic Maxwell Equations

M.E. Tobar, B.T. McAllister, M. Goryachev arXiv: 1809.01654v11

$$\vec{\nabla}\cdot\vec{D}=\rho_f+g_{a\gamma\gamma}\sqrt{\frac{\epsilon_0}{\mu_0}}\vec{B}\cdot\vec{\nabla}a,$$

$$\vec{\nabla}\times\vec{H}=\vec{J}_f+\frac{\partial\vec{D}}{\partial t}-g_{a\gamma\gamma}\sqrt{\frac{\epsilon_0}{\mu_0}}\left(\vec{B}\frac{\partial a}{\partial t}+\vec{\nabla}a\times\vec{E}\right),$$

$$\vec{\nabla}\cdot\vec{B}=0,$$

$$\vec{\nabla}\times\vec{E}=-\frac{\partial\vec{B}}{\partial t},$$

Constitutive Relations

$$\vec{H}=\vec{B}/\mu_0-\vec{M}$$

$$\vec{D}=\epsilon_0\vec{E}+\vec{P}$$

Axion field

$$a(t,\vec{r})=a_0\cos(\vec{k}_a\cdot\vec{r}-\omega_a t)$$

Axionic Maxwell Equations

In the absence of a spatial dependence

$$\vec{\nabla} \times \vec{H} = \vec{J}_f + \frac{\partial \vec{D}}{\partial t} + \vec{J}_a$$

where we have an effective current given by

$$\vec{J}_a = -g_{a\gamma\gamma}\sqrt{\frac{\epsilon_0}{\mu_0}}\vec{B}\frac{\partial a}{\partial t}$$

Axionic Maxwell Equations

Alternatvely we can rewrite these equations to have the same form as the original Maxwell equations but with new fields and new constitutive relations.

$$\vec{\nabla} \cdot \vec{D}_T = \rho_f ,$$

$$\vec{\nabla} \times \vec{H}_T - \frac{\partial \vec{D}_T}{\partial t} = \vec{J}_f ,$$

$$\vec{\nabla} \cdot \vec{B} = 0,$$

$$\vec{\nabla} \times \vec{E} + \frac{\partial \vec{B}}{\partial t} = 0$$

$$\vec{D}_T = \epsilon_0 \vec{E} + \vec{P} + \vec{P}_{aB} \text{ where } \vec{P}_{aB} = -g_{a\gamma\gamma} \sqrt{\frac{\epsilon_0}{\mu_0}} (a\vec{B}),$$

$$\vec{H}_T = \frac{\vec{B}}{\mu_0} - \vec{M} - \vec{M}_{aE} \text{ where } \vec{M}_{aE} = -g_{a\gamma\gamma} \sqrt{\frac{\epsilon_0}{\mu_0}} (a\vec{E}).$$

M.E. Tobar, B.T. McAllister, M. Goryachev arXiv: 1809.01654v11

Experimental Searches

Source \ Coupling	*Photons*	*Fermions*	*nEDMs*
Dark matter	*ADMX, CAPP, MADMAX, DM Radio, …*	*QUAX-ae, GNOME, CASPEr-wind, …*	*CASPEr-electric, srEDM, …*
Solar	*CAST, IAXO*		
Laboratory	*ALPS (II)*	*ARIADNE*	

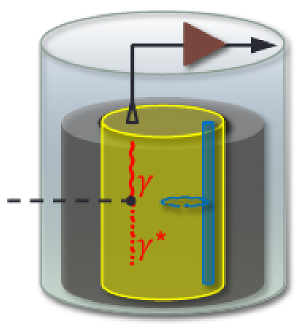

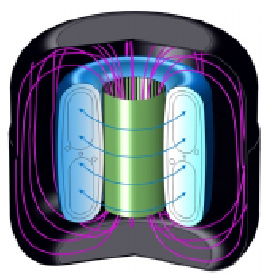

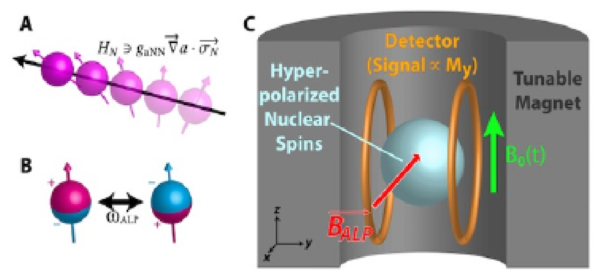

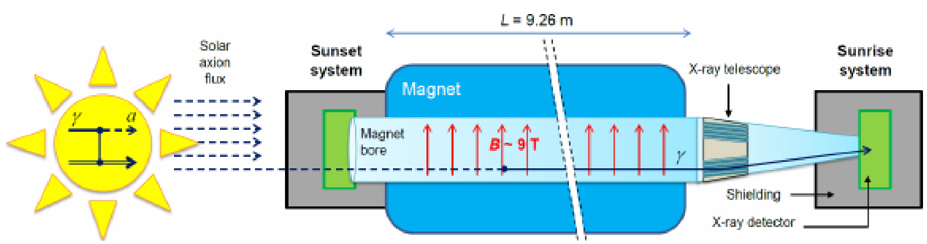

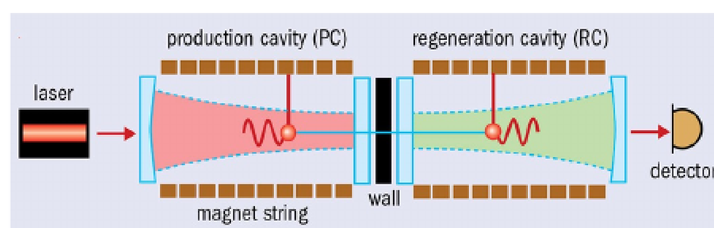

S. Yun, 17th Patras Workshop on axions, WIMPs and WISPs, 2022, Mainz.

Experimental Searches

Source \ Coupling	Photons	Fermions	nEDMs
Dark matter	*ADMX, CAPP, MADMAX, DM Radio, …*	*QUAX-ae, GNOME, CASPEr-wind, …*	*CASPEr-electric, srEDM, …*
Solar	*CAST, IAXO*		
Laboratory	*ALPS (II)*	*ARIADNE*	

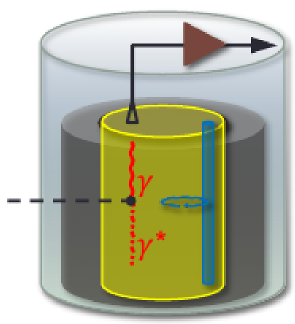

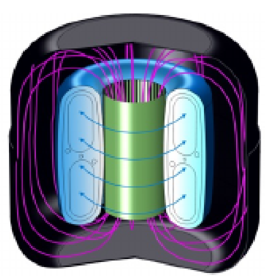

We are focussing here, but nothing we have looked at so far tells us the mass of the axion…

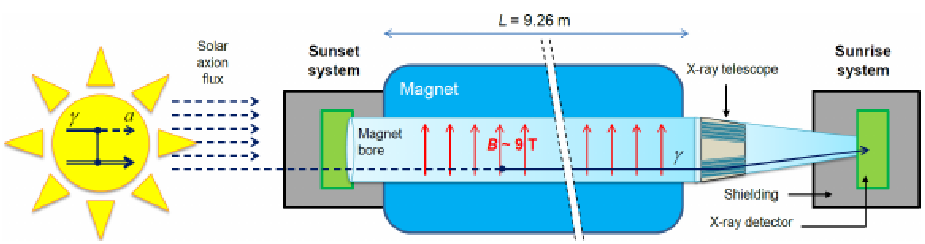

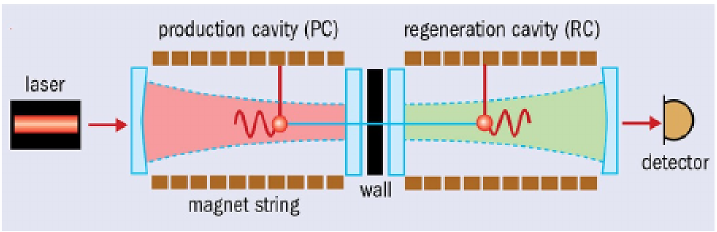

Theoretical predictions of QCD axion dark matter mass

Predictions of the axion mass come from considering axion production mechanisms in the early universe.

- If $U(1)_{PQ}$ unbroken at end of inflation:
  - Decay of strings, solitons and domain walls produces axions
  - Models tend to predict masses around 100 μeV or above
- If $U(1)_{PQ}$ broken before inflation:
  - Non-thermal production via misalignment mechanism
  - Masses far below 100 μeV possiblese.

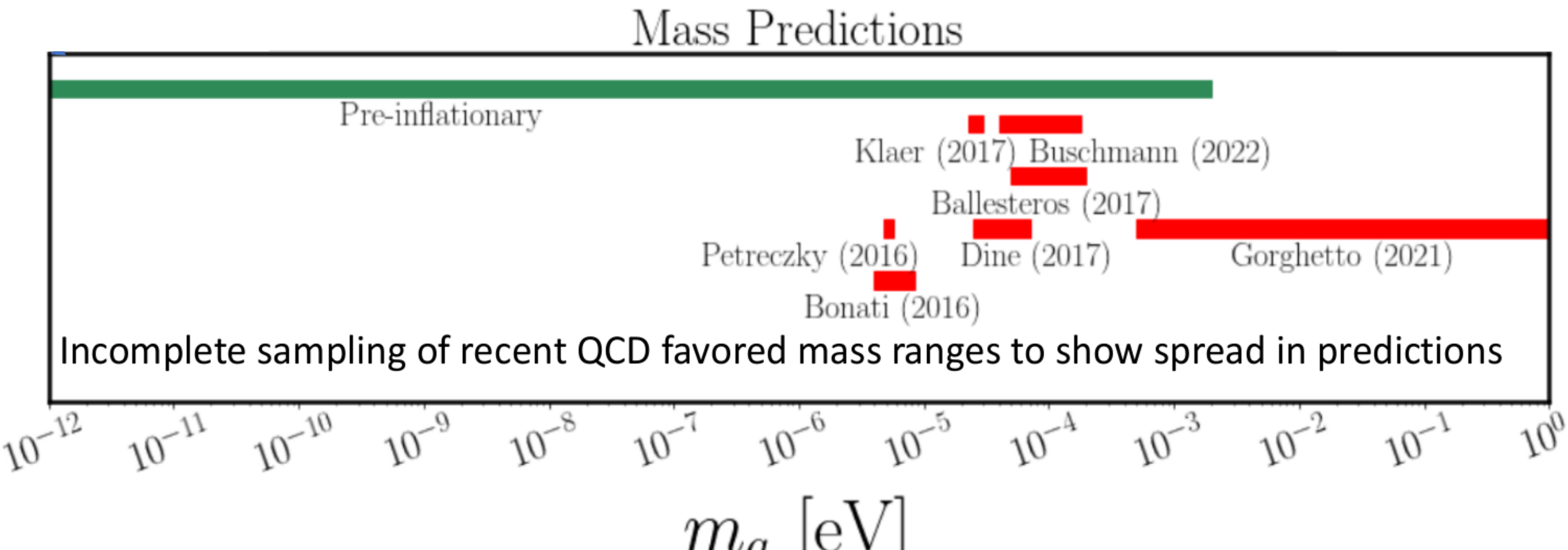

Dark Matter Candidates ***and Anomalies***

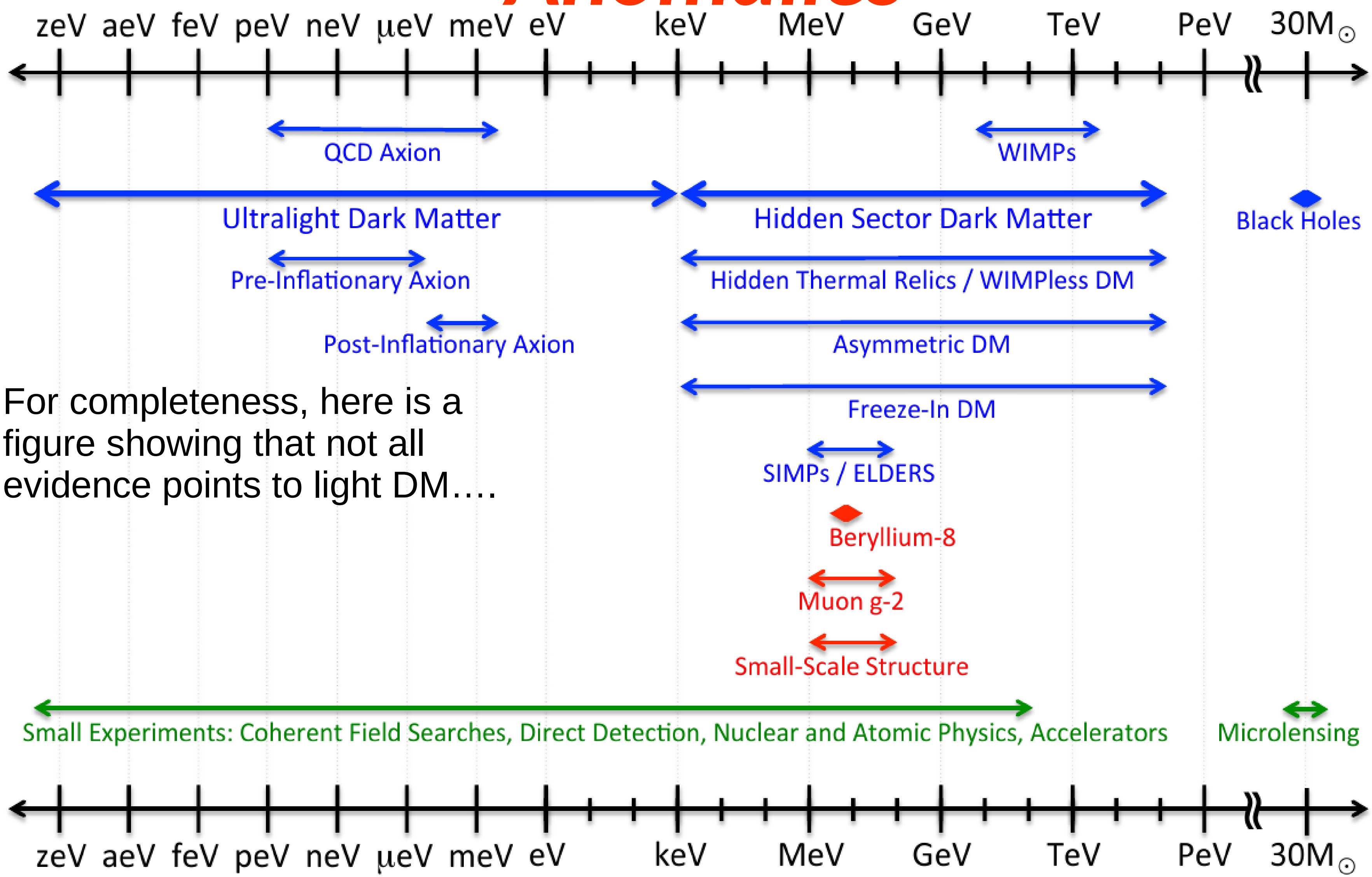

For completeness, here is a figure showing that not all evidence points to light DM….

Battaglieri et al, arxiv, 1707.04591

Theoretical predictions of QCD axion dark matter mass

Predictions of the axion mass come from considering axion production mechanisms in the early universe

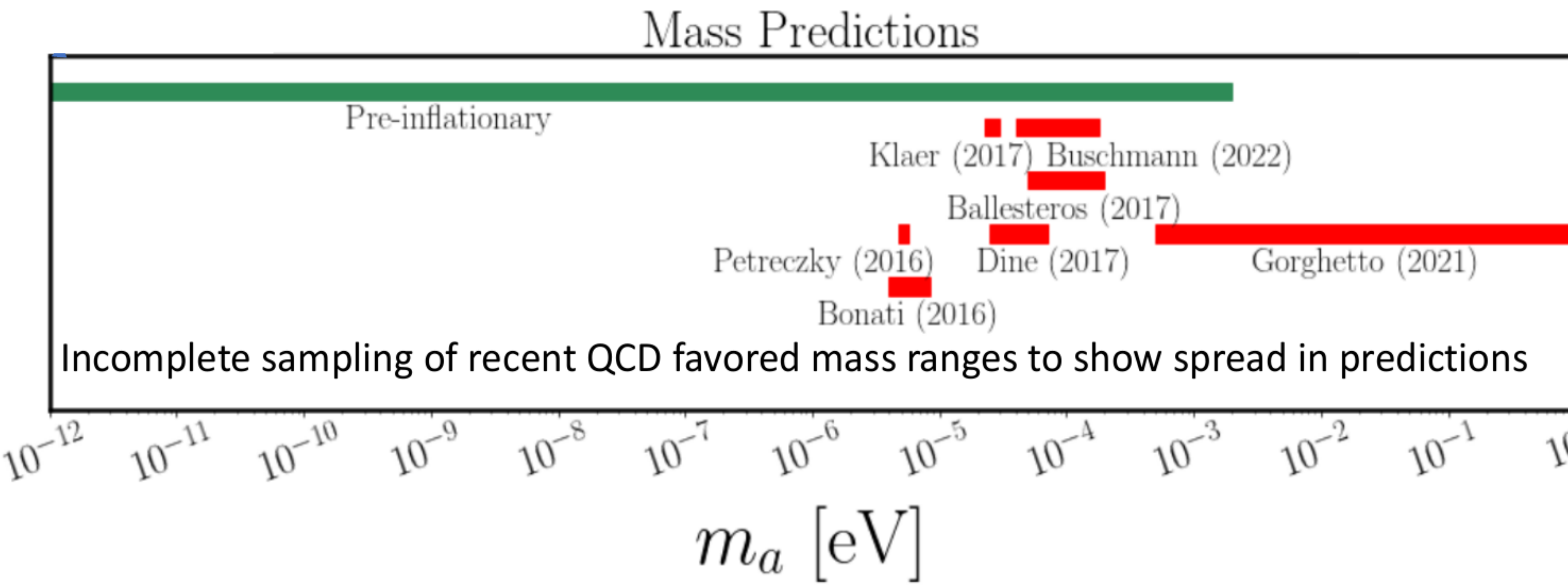

Now that we have a favoured mass window, can we say anything about the coupling strength?

Back to the Primakoff Effect

Consider coupling of axion to e/m fields

$$\mathscr{L}_{a\gamma\gamma} = g_{a\gamma\gamma} a \mathbf{E} \cdot \mathbf{B}$$

The effective coupling **depends on the particles to which the axion can couple directly**

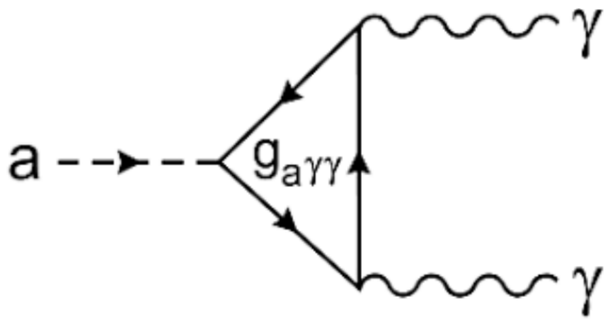

The axion mechanism gives a dimension-5 term.

$$\frac{a}{f_a} G^{\mu\nu} \tilde{G}_{\mu\nu}$$

UV-completion ⇒ 4-dim effective field theory.

QCD Axion Models

Models can either contain only SM fermions

- The original PQ solution with 2 Higgs bosons (“Visible axion”)
- DFSZ (Dine, Fischler, Srednicki, Zhitnitsky 1980)

...or BSM fermions

- KSVZ (Kim, Shifman, Vainshtein, Zakharov 1980)

Gives model-dependent couplings

$$g_{a\gamma\gamma} \approx \frac{\alpha}{2\pi}\left[\frac{1}{f_{\mathrm{UV}}} - \frac{1.92}{f_a}\right] \qquad g_{a\gamma\gamma} = \frac{g_\gamma \alpha}{\pi f_a}$$

$$m_a = \frac{\sqrt{m_u m_d}}{m_u + m_d}\frac{f_\pi m_\pi}{f_a} \qquad m_a \approx 6 \times 10^{-6}\,\mathrm{eV}\left(\frac{10^{12}\,\mathrm{GeV}}{f_a}\right)$$

QCD Axion Models

Models can either contain only SM fermions
- The original PQ solution with 2 Higgs bosons (“Visible axion”)
- DFSZ (Dine, Fischler, Srednicki, Zhitnitsky 1980)

...or BSM fermions
- KSVZ (Kim, Shifman, Vainshtein, Zakharov 1980)

Gives model-dependent couplings

$$g_{a\gamma\gamma} \approx \frac{\alpha}{2\pi}\left[\frac{1}{f_{\mathrm{UV}}} - \frac{1.92}{f_a}\right] \qquad g_{a\gamma\gamma} = \frac{g_\gamma \alpha}{\pi f_a}$$

$$m_a = \frac{\sqrt{m_u m_d}}{m_u + m_d}\frac{f_\pi m_\pi}{f_a} \qquad m_a \approx 6\times 10^{-6}\,\mathrm{eV}\left(\frac{10^{12}\,\mathrm{GeV}}{f_a}\right)$$

$$\therefore g_{a\gamma\gamma} \propto m_a$$

See for example PoS(TASI2018)004

Experimental Constraints on Axions

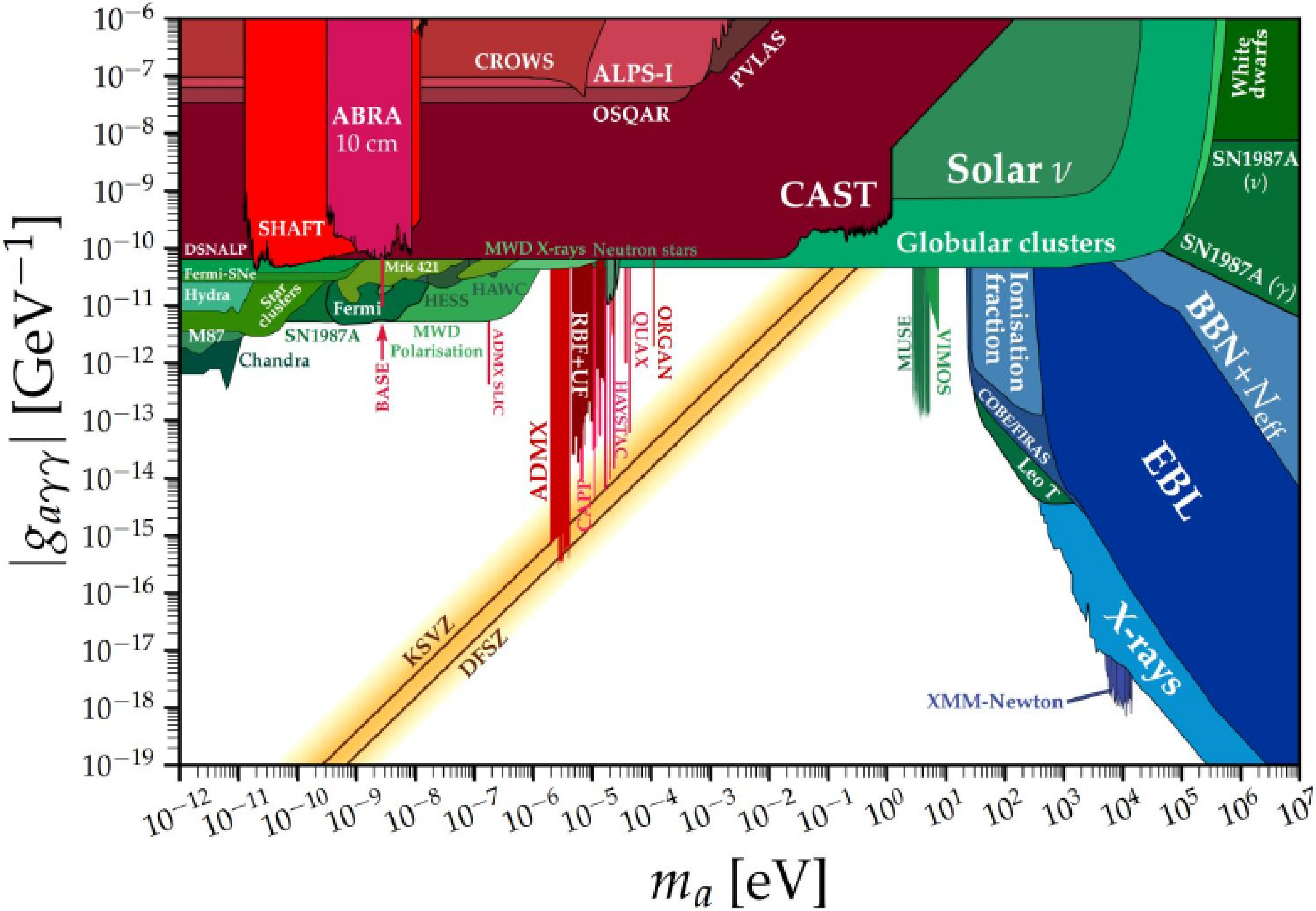

https://github.com/cajohare/AxionLimits

Experimental Constraints on Axions

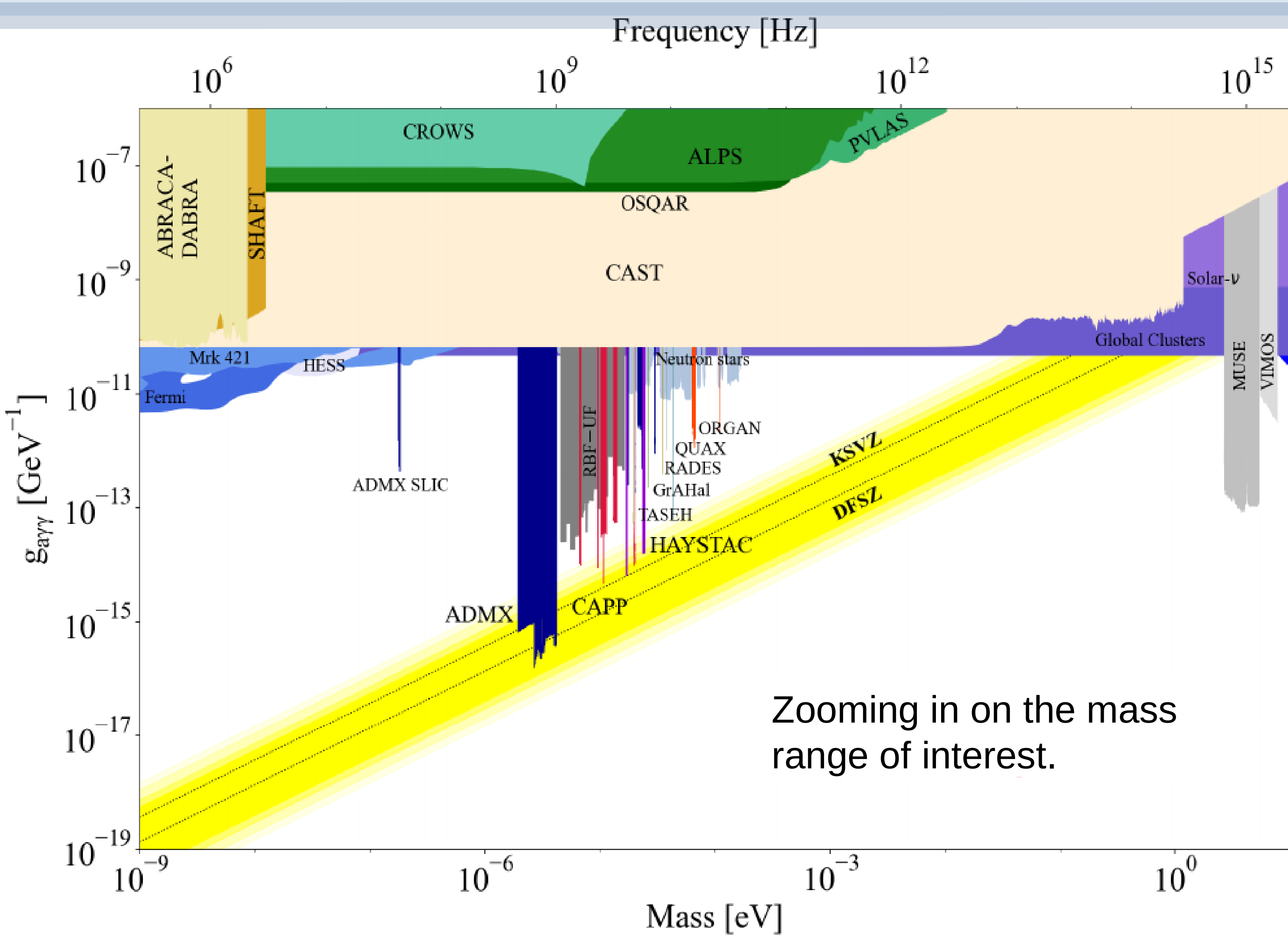

Zooming in on the mass range of interest.

Cavity Haloscopes for Axion Detection

The **axion haloscope** is a resonant axion search using microwave cavities

The axion frequency is unknown – the resonant cavity must be tunable for a range of frequencies

1. **Cavity** has various resonant modes which enhances the signal power of converted photon
2. **Tuning rods** are required to change the resonant frequency of cavity, usually copper or dielectric
3. External static **magnetic field** allows axion to photon conversion
4. **Antenna** used to receive signal (Signal power depends on coupling)
5. **JPA** and other amplifiers in and outside cryostat amplify the signal
6. Signal is studied using a **digitizer** in the frequency domain
7. Experiments are conducted inside a cryostat and dilution fridge at **low temperatures** to reduce noise power

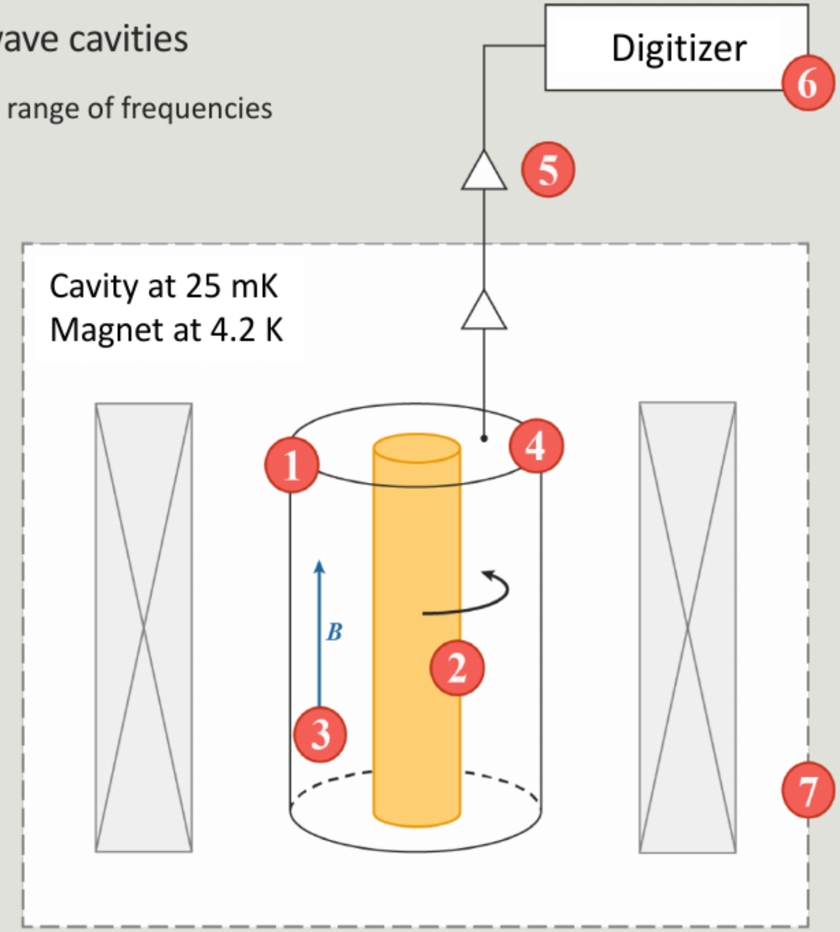

Cavity Haloscopes for Axion Detection

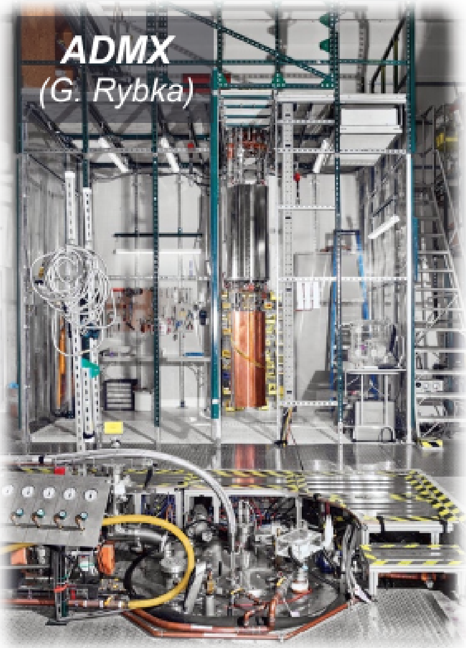

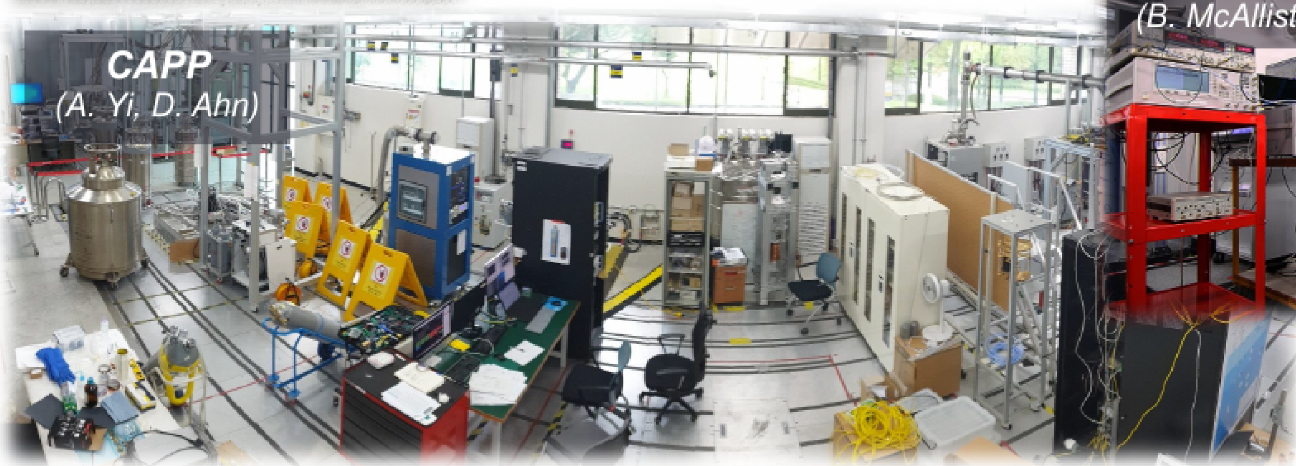

Axion Haloscopes

Power deposited in a resonant detector cavity

$$P_{a\to\gamma} = \frac{\omega_c U}{Q_c} = \frac{\omega_c}{Q_c}\left(\int d^3r \left\langle \frac{\boldsymbol{E}_a^2 + \boldsymbol{B}_a^2}{2} \right\rangle\right)$$

where U is the stored energy and Q is the quality factor

$$a(t) = \sqrt{T}\int_{-\infty}^{+\infty} \frac{d\omega}{2\pi}\mathcal{A}(\omega)e^{-i\omega t}$$

$$\mathcal{A}(\omega) = \frac{1}{\sqrt{T}}\int_{-T/2}^{T/2} dt\, a(t)e^{i\omega t}.$$

$$\langle a^2(t)\rangle = \frac{1}{T}\int_{-T/2}^{T/2} dt\, a^2(t) = \int_{-\infty}^{+\infty}\frac{d\omega}{2\pi}|\mathcal{A}(\omega)|^2$$

Axion Haloscopes

Power deposited in a resonant detector cavity

$$P_{a\to\gamma} = \frac{\omega_c U}{Q_c} = \frac{\omega_c}{Q_c}\left(\int d^3r \left\langle \frac{\boldsymbol{E}_a^2 + \boldsymbol{B}_a^2}{2} \right\rangle\right)$$

where U is the stored energy and Q is the quality factor

If the cavity is tuned to the axion energy then $\omega = m_a(1 + \langle v^2\rangle/6) \equiv \omega_a$

assuming that the axion DM is thermalised.

$$|\mathcal{A}(\omega)|^2 = \frac{\omega_a \rho_{.}}{m_a^2 Q_a} \frac{1}{(\omega - \omega_a)^2 + (\omega_a/2Q_a)^2}$$

where the axion quality factor is just given by

$$Q_a \equiv \frac{\omega_a}{\Delta\omega} \simeq \frac{m_a}{m_a\langle v^2\rangle/3} \sim 3 \times 10^6$$

arXiv:1403.1576v1 and JCAP03 (2020) 066

Axion Haloscopes

arXiv:1403.1576v1 and JCAP03 (2020) 066

Power deposited in a resonant detector cavity

$$P_{a\to\gamma} = \frac{\omega_c U}{Q_c} = \frac{\omega_c}{Q_c}\left(\int d^3r \left\langle \frac{\boldsymbol{E}_a^2 + \boldsymbol{B}_a^2}{2} \right\rangle\right)$$

where U is the stored energy and Q is the quality factor

We can now use the results along with

$$\begin{aligned} \boldsymbol{E}_a(\boldsymbol{r},\omega) &= g_{a\gamma\gamma}\mathcal{A}(\omega,\omega_a)\boldsymbol{B}_0\left[1+\mathcal{F}(\omega,\omega_c)\mathcal{T}(\boldsymbol{r}\omega)\right] \\ &\approx g_{a\gamma\gamma}\mathcal{A}(\omega,\omega_a)\boldsymbol{B}_0\mathcal{F}(\omega,\omega_c)\mathcal{T}(\boldsymbol{r}\omega), \end{aligned}$$

where the cavity enhancement factor is

$$\mathcal{F}(\omega,\omega_c) = \frac{1}{(\omega-\omega_c) + i\omega_c/2Q_c}$$

and

$\nabla^2\mathcal{T}(\boldsymbol{r}\omega) = \omega^2\mathcal{T}(\boldsymbol{r}\omega)$ is related to the spatial 'form factor' C by $\int_V \mathcal{T}^2(\boldsymbol{r}\omega)d^3r = CV/\omega$

to obtain $P_{a\to\gamma} = g^2_{a\gamma\gamma}\frac{\rho_a}{m_a^2}B_0^2 V\omega_0 C Q_c$ assuming $Q_c \ll Q_a$

Axion Haloscopes

Power deposited in a resonant detector cavity

$$P_{a\to\gamma} = \frac{\omega_c U}{Q_c} = \frac{\omega_c}{Q_c}\left(\int d^3r \left\langle \frac{\boldsymbol{E}_a^2 + \boldsymbol{B}_a^2}{2} \right\rangle\right)$$

where U is the stored energy and Q is the quality factor

$$P_{a\to\gamma} = g_{a\gamma\gamma}^2 \frac{\rho_a}{m_a^2} B_0^2 V \omega_0 C Q_c$$

$$\frac{\left|\int_V \mathbf{E_c}\cdot\mathbf{B_0} d^3x\right|^2}{\int_V \epsilon(x)|\mathbf{E_c}|^2 d^3x \int_V |\mathbf{B_0}|^2 d^3}$$

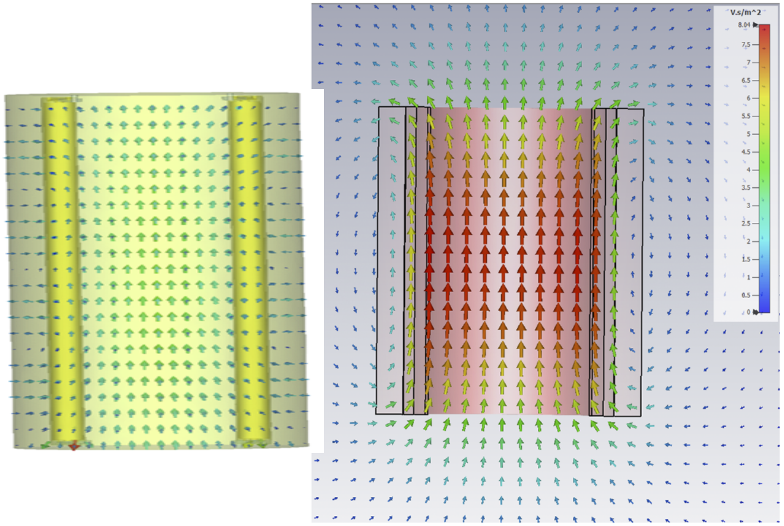

Review of Scientific Instruments 92, 124502 (2021)

arXiv:1403.1576v1 and JCAP03 (2020) 066

Axion Haloscopes

Power deposited in a resonant detector cavity

$$P_{a\to\gamma} = \frac{\omega_c U}{Q_c} = \frac{\omega_c}{Q_c}\left(\int d^3r \left\langle \frac{\boldsymbol{E}_a^2 + \boldsymbol{B}_a^2}{2} \right\rangle\right)$$

where U is the stored energy and Q is the quality factor

$$P_{a\to\gamma} = g_{a\gamma\gamma}^2 \frac{\rho_a}{m_a^2} B_0^2 V \omega_0 C Q_c$$

$$Q_c = \frac{1}{1+R/L}\frac{R}{\delta}$$

If we are extracting power then this should be the loaded Q. The quality factor of the receiver is given by Q_c/β where β is the receiver coupling strength.

arXiv:1403.1576v1 and JCAP03 (2020) 066

Axion Haloscopes

Power deposited in a resonant detector cavity

$$P_{a\to\gamma} = \frac{\omega_c U}{Q_c} = \frac{\omega_c}{Q_c}\left(\int d^3r \left\langle \frac{\boldsymbol{E}_a^2 + \boldsymbol{B}_a^2}{2} \right\rangle\right)$$

where Q is the quality factor

$$P_{a\to\gamma} = g_{a\gamma\gamma}^2 \frac{\rho_a}{m_a^2} B_0^2 V \omega_0 C Q_c$$

Noise is thermal

$$\frac{S}{N} = \frac{P_{a\to\gamma}}{k_B T_{\text{sys}}}\sqrt{\frac{t}{b}}$$

$$P_n = k_B T b \left(\frac{hf/k_B T}{\exp(hf/k_B T) - 1} \right) + \frac{hfb}{2}$$

$$\frac{df}{dt} = g_{a\gamma\gamma}^4 \frac{\rho_a^2}{m_a^2} \frac{1}{\text{SNR}^2} \frac{B_0^4 V^2 C^2}{k_B^2 T_{\text{sys}}^2} Q_c$$

Review of Scientific Instruments 92, 124502 (2021)

Haloscope Figures of Merit

$$P_{a\to\gamma\gamma} = g_{a\gamma\gamma}^2 \frac{\rho_a}{m_a^2} B_0^2 V \omega_0 C Q_c$$

$$\frac{df}{dt} = g_{a\gamma\gamma}^4 \frac{\rho_a^2}{m_a^2} \frac{1}{\mathrm{SNR}^2} \frac{B_0^4 V^2 C^2}{k_B^2 T_{\mathrm{sys}}^2} Q_c$$

$$GT_{\mathrm{equiv}} = G(T + T_a)$$

$$T_{\mathrm{equiv}} = \alpha T + T_\alpha (1 - \alpha)$$

Dielectric Haloscopes

- MAgnetized Disk-and-Mirror Axion eXperiment

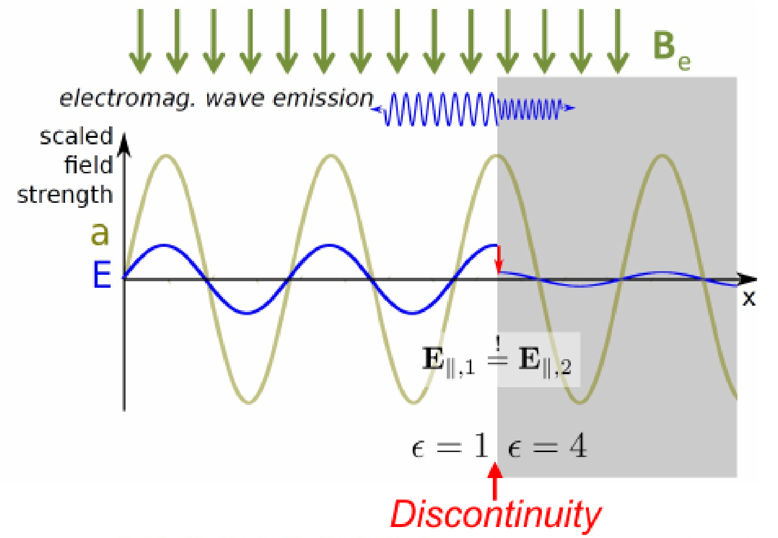

$$P_{a\gamma\gamma} = 1.6\times10^{-22}\, W \left(\frac{\beta^2}{5\times10^4}\right)\left(\frac{A}{1\, m^2}\right) \left(\frac{B_e}{10\, T}\right)^2 \left(\frac{C_{a\gamma}}{1}\right)^2 \left(\frac{\rho_a}{0.45\, GeV cm^{-3}}\right)$$

- Frequency: distance b/w disks
- 40–400 μeV (10–100 GHz)
- Suitable for high mass searches

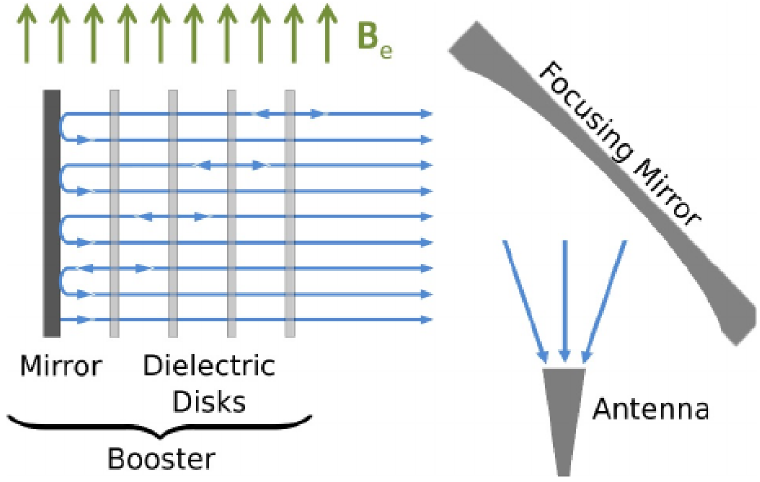

Boosting factor β

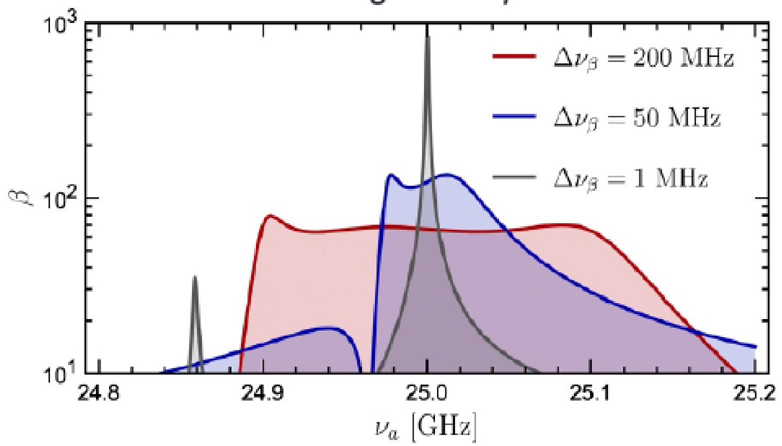

Behaviour at dielectric interface

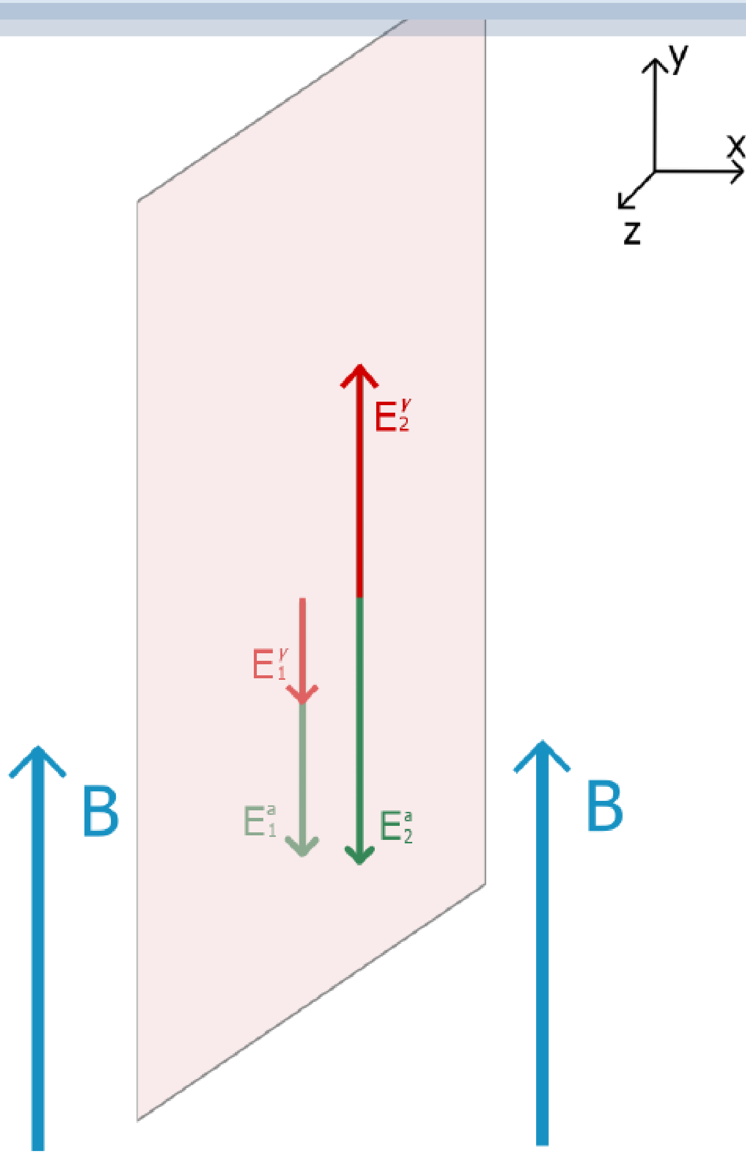

$$
\begin{aligned}
E_1^\gamma =& (E_2^a - E_1^a)\frac{\epsilon_2 n_1}{\epsilon_1 n_2 + \epsilon_2 n_1} \\
E_2^\gamma =& (E_1^a - E_2^a)\frac{\epsilon_1 n_2}{\epsilon_1 n_2 + \epsilon_2 n_1} \\
H_1^\gamma =& H_2^\gamma = (E_1^a - E_2^a)\frac{\epsilon_1 \epsilon_2}{\epsilon_1 n_2 + \epsilon_2 n_1}
\end{aligned}
$$

$E_{1,2}^{\gamma}$ and $H_{1,2}^{\gamma}$ correspond to a propagating wave

$E_{1,2}^{a}$ are electric fields induced by the axion field

Alexander J. Millar et al JCAP01(2017)061

Behaviour at dielectric interface

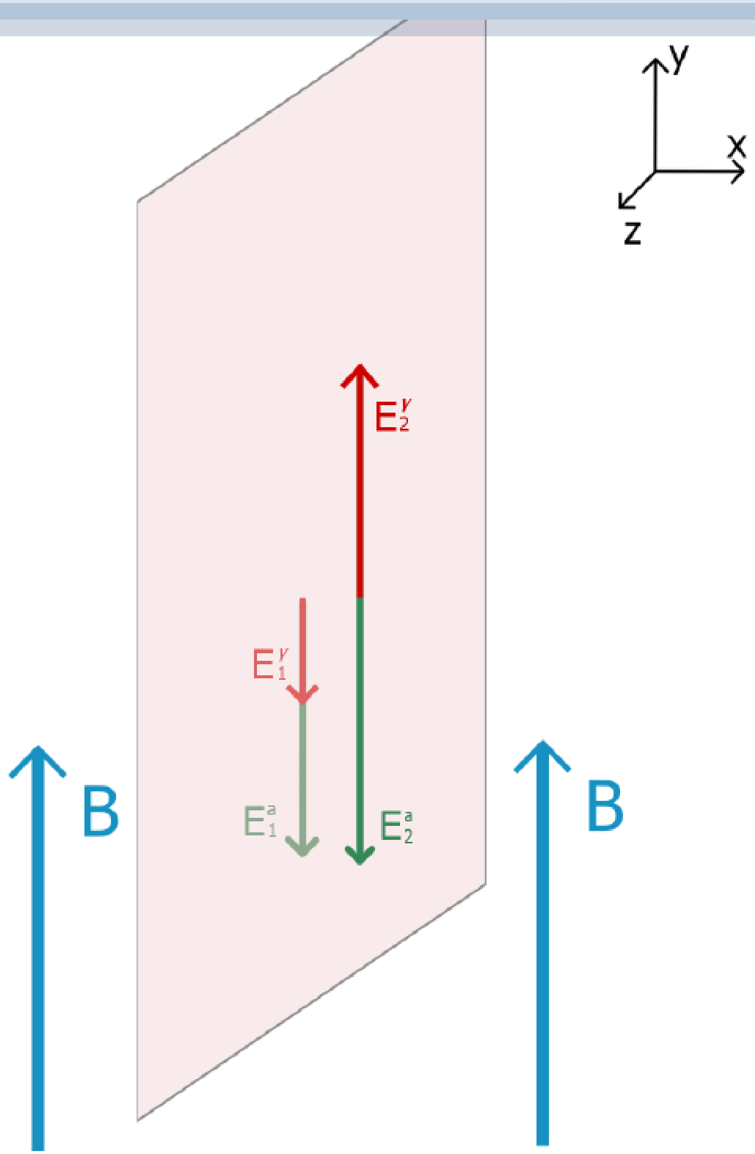

$$E_1^\gamma = (E_2^a - E_1^a)\frac{\epsilon_2 n_1}{\epsilon_1 n_2 + \epsilon_2 n_1}$$
$$E_2^\gamma = (E_1^a - E_2^a)\frac{\epsilon_1 n_2}{\epsilon_1 n_2 + \epsilon_2 n_1}$$
$$H_1^\gamma = H_2^\gamma = (E_1^a - E_2^a)\frac{\epsilon_1 \epsilon_2}{\epsilon_1 n_2 + \epsilon_2 n_1}$$

Poynting fluxes

$$S_1 = -\frac{E_0^2}{2n_1^2}\left(\frac{1}{n_2} - \frac{1}{n_1}\right)\left[\frac{n_1}{n_2} - 2\sin^2\left(\frac{n_1 \omega x}{2}\right)\right]$$
$$S_2 = \frac{E_0^2}{2n_2^2}\left(\frac{1}{n_2} - \frac{1}{n_1}\right)\left[2\sin^2\left(\frac{n_2 \omega x}{2}\right) - \frac{n_2}{n_1}\right]$$

Behaviour at dielectric interface

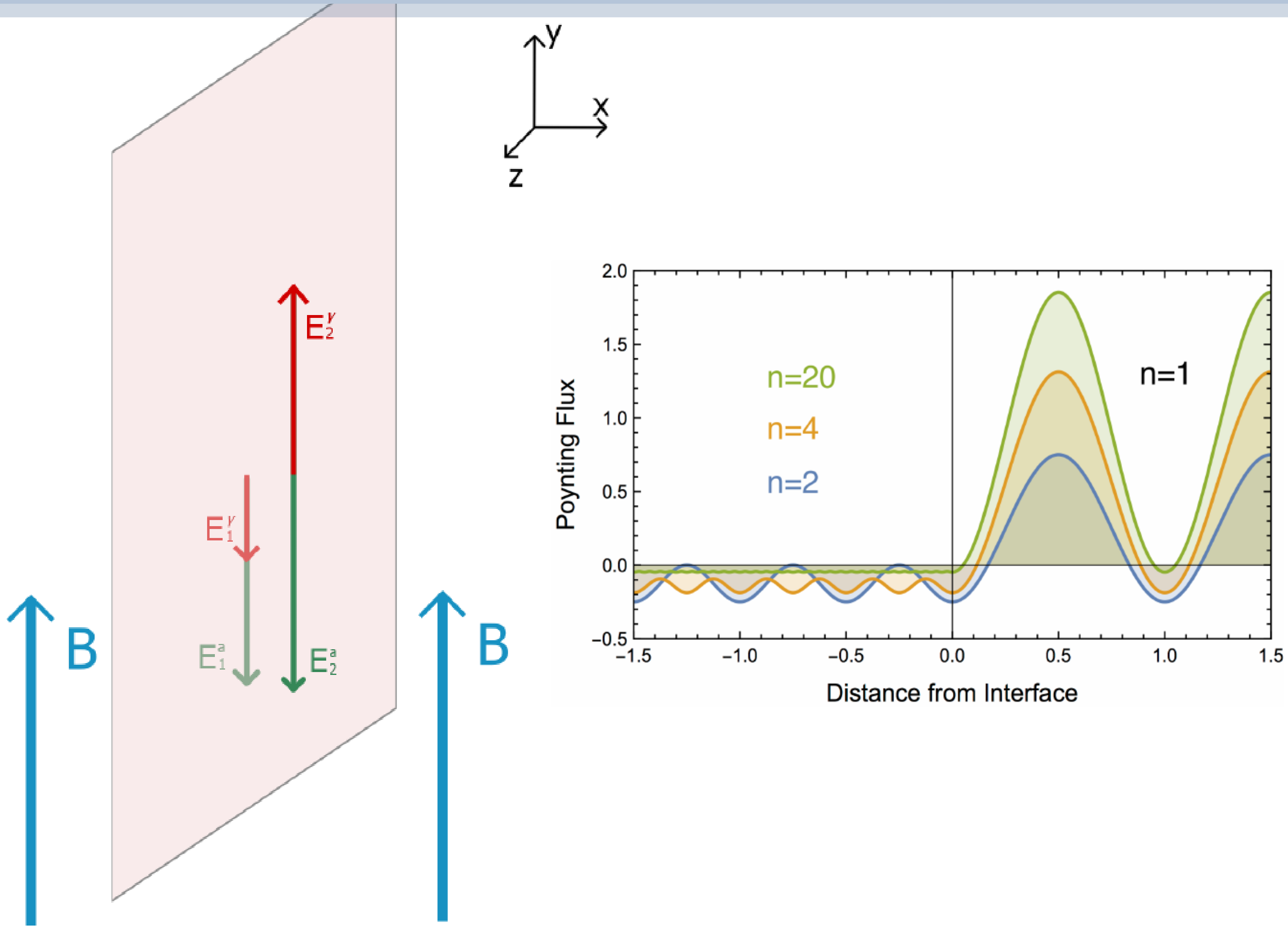

Enhancing Form Factors

- *Periodic planes for short wavelength*
  - *Non-vanishing form factors*

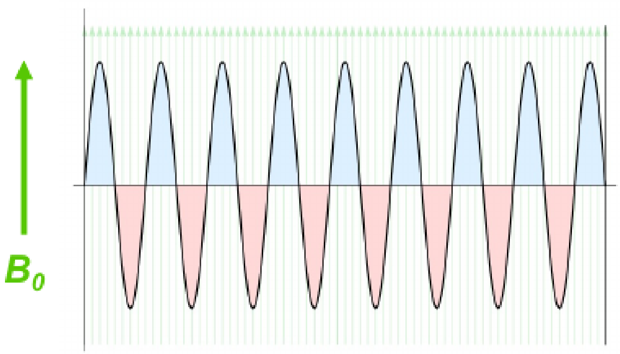

Form factor vanishes w/ a static B field

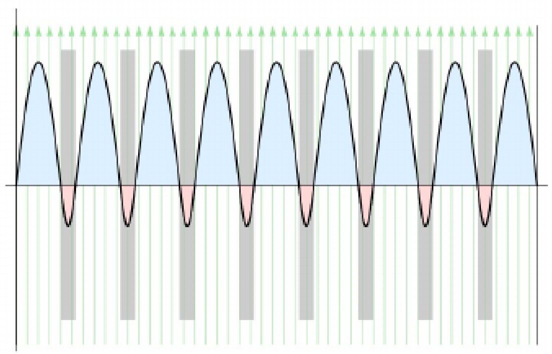

Suppressing negative E field (dielectric planes)

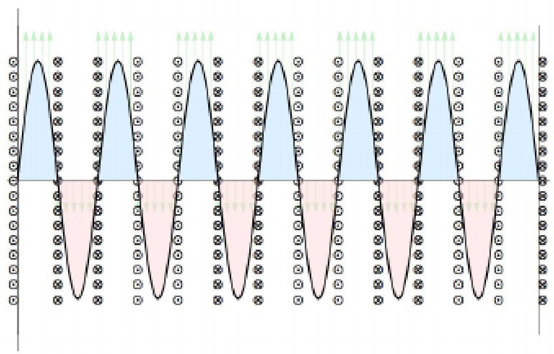

Producing alternating B field (wire planes)

$$C_{mnp} = \frac{\left| \int \vec{E}_c \cdot \vec{B}_0 \, dV \right|^2}{\int \varepsilon \left| \vec{E}_c \right|^2 dV \int \left| \vec{B}_0 \right|^2 dV}$$

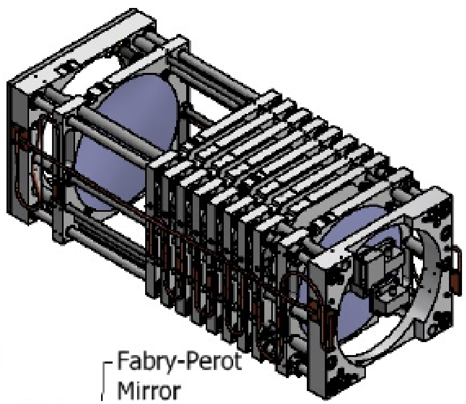

Electric Tiger

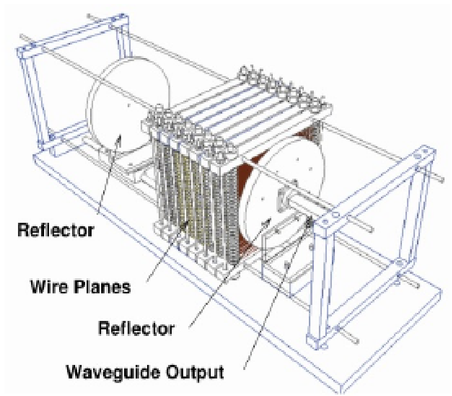

ORPHEUS

*PRD **91**, 011701 (2015)*

Metamaterials and Photonics

S. Yun, 17th Patras Workshop on axions, WIMPs and WISPs, 2022, Mainz.

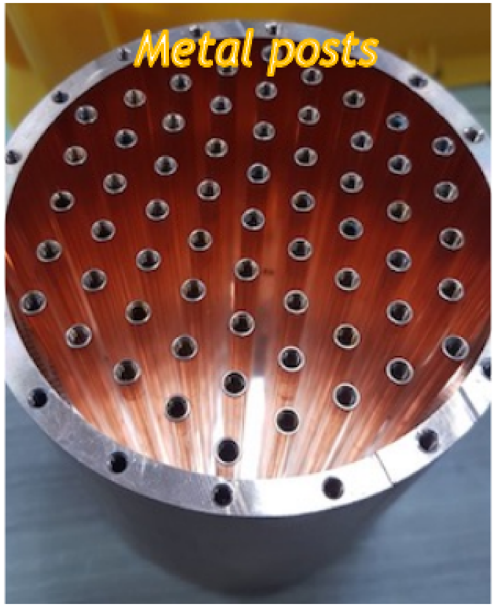

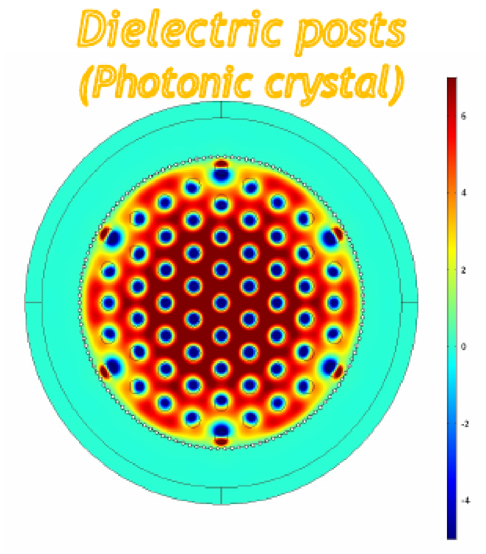

Metal wires	Metal posts	Dielectric posts
C = 0.81 (boundary effect)	C = 0.76	C = 0.23
$Q = 9.6 \times 10^3$	$Q = 1.7 \times 10^4$	$Q = 1.8 \times 10^5$
Density ~3 wires/cm^2	Density ~1 posts/cm^2	Density ~1 posts/cm^2
Plasma concept	Higher Q, Less density	Even higher Q

Summary

- A reminder of the motivation for dark matter
- Review of dark matter candidates
- WISPs / FISPs (Feebly-interacting sub-eV particles)
- QCD Axions
- Axion couplings
- The axion-photon coupling
- Axion experimental detection techniques
- Axion haloscopes

- See Ed Daw’s lecture later in the week for a quantum systems view of the detectors coupled to axion haloscopes.

Backup Slides

BREAD Concept

“coaxial dish antenna”

[Liu *et al*, BREAD collab., arXiv:2111.12103, PRL 128 (2022) 131801]

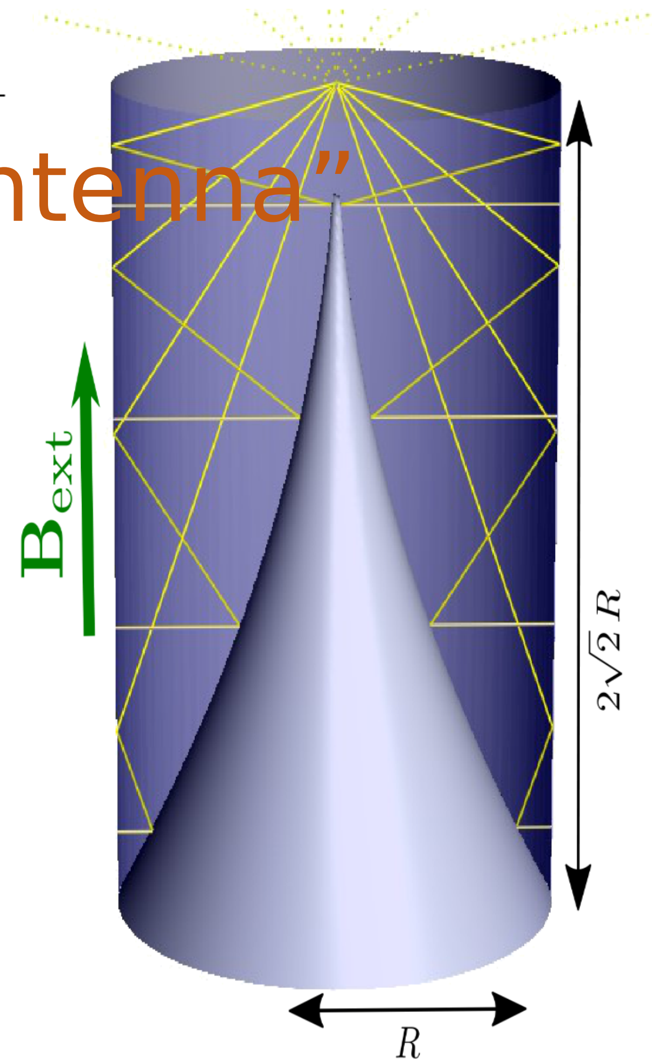

in solenoid magnet

(e.g.,MRI)

$$P_{sig} = 1 \cdot 10^{-25}\,W \cdot \left(\frac{A}{10\,m^2}\right)\left(\frac{B_{\parallel}}{10\,T}\right)^2 \left(\frac{\rho_{DM}}{0.45\,GeV\,cm^{-3}}\right)\left(\frac{g_{a\gamma\gamma}}{3.9 \cdot 10^{-16} \geq V^{-1}}\right)^2 \left(\frac{1\,\mu eV}{m_a}\right)^2$$

Static-field Haloscope:

e.g. ADMX

$$\omega_{\text{sig}} = m_a \sim V^{-1/3}$$

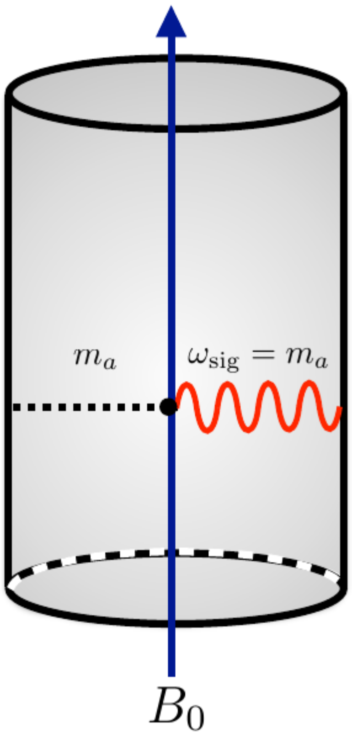

LC Resonator:

$$\omega_{\text{sig}} = m_a = \omega_{\text{LC}}$$

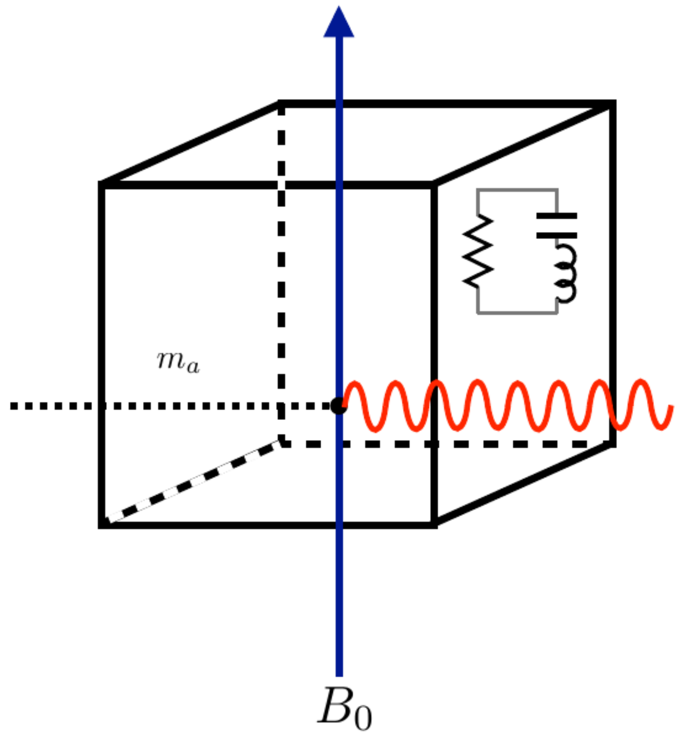

Heterodyne Resonator:

$$\omega_{\text{sig}} \sim \omega_0 \pm m_a \sim V^{-1/3}$$

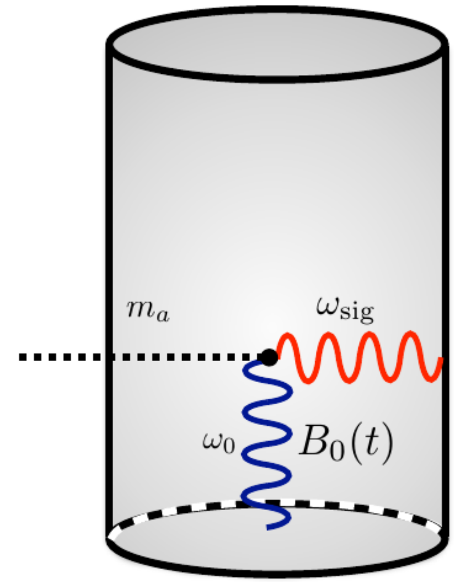

JHEP 07 (2020) 088, hep-ph/1912.11048
A. Berlin, R. T. D'Agnolo, SARE, P. Schuster, N. Toro, C. Nantista, J. Neilson, S. Tantawi, K. Zhou

Also: R. Lasenby hep-ph/1912.11467

Sebastian A. R. Ellis

IPhT, CEA Saclay

BRASS-p Setup